CDF/ANAL/EXOTIC/CDFR/4976
Version 2.1
May 8, 1999

A Search for Physics Beyond the Standard Model in Inclusive Photon-Lepton Events I: Standard Model Expectations

Troy Andre, Jeff Berryhill, Ray Culbertson, Henry Frisch, Nancy Lai, Pasha Murat, and Peter Wilson

Abstract

Motivated by the $ee\gamma\gamma\not\!\!E_{\mathrm{T}}$ event, we have searched in the inclusive channels $e\gamma$ and $\mu\gamma$ for a signal beyond that predicted in the Standard Model. Such a signature is natural in gauge-mediated supersymmetry models with either a long-lived heavy particle and R-parity conservation, or with R-parity violation. This signature could also arise from more conventional models from photino-chargino decays, or from any other process that produces a charged and a neutral particle that cascade decay to the SM vector bosons W and γ, for example. The analysis presented here is intended as the final treatment of the analysis presented in CDF3555 and CDF3851: the main differences are that we use the final Berryhill photon identification cuts with the Wilson isolation corrections, we have revertexed all events with the vertex determined by the lepton track, and we have removed the missing Et requirement so that the initial signature is solely a high-P_T photon and a high-P_T central electron or muon, where high-P_T is greater than 25 GeV. This note describes the Standard Model expectations in these channels; the data are described in CDFnote CDF4977.

Contents

1 Introduction

The $ee\gamma\gamma\not\!\!E_t$ event motivated two complementary searches for related events; we have searched for events in the diphoton ($\gamma\gamma$)[1] and lepton-photon-missing transverse energy ($\ell\gamma\not\!\!E_t$) channels[2, 3]. Both searches, $\gamma\gamma$, and $\ell\gamma\not\!\!E_t$, were based on the hypothesis that the $ee\gamma\gamma\not\!\!E_t$ event originated from the decay of a pair of new particles, each of which yielded an electron, photon, and $\not\!\!E_{\rm T}$[4]. The diphoton search has been completed, and we have returned to the lepton-photon search with a better understanding of the subtle details of photon identification and a new set of tools (such as a rigorous $W+\gamma$ Monte Carlo and a fake-rate methodology[1]) with the intent of completing it for publication.

The analysis is described in two CDF notes. This note describes the Standard Model expectations; CDF4977[5] describes the results from the data. So that each note stands by itself,we have duplicated parts of the sections on theoretical motivation and the selection criteria; however the two notes are made to be read in conjunction, with this one being the first of the two.

1.1 Signature and Motivation

The signature of a high-P_T photon, a high-P_T lepton, and missing E_T can arise from a number of currently popular models, as well as being an archetypal search mode for more fundamental reasons: it contains one neutral vector boson and, possibly, a decay product of either a second vector boson or of a new heavy particle (such as a slepton, chargino or a heavy lepton) that couples to e, μ, or τ.

1.2 Specific Models

In models constructed with a photino as the NLSP and a Higgsino LSP, the photino $\tilde{\chi}_2^0$ decays via a loop into $\gamma\tilde{\chi}_1^0$[6, 7]. The decay of a pair of selectrons or gauginos would thus produce the $ee\gamma\gamma\not\!\!E_t$ signature as shown in Figure 1. Such models would, in general, produce more events with one photon than with two. Further, chargino-neutralino production, or a cascade decay of squarks and gluinos through charginos and neutralinos, would produce final states with a lepton, photon, and missing E_T.

In contrast, gauge-mediated models of supersymmetry breaking, in which the LSP is the gravitino, $\tilde{G}$, are predicted to give signatures (in general) in which all final states end up with two photons[7, 8], as sparticles are made in pairs, and each decay chain results in a decay of an NLSP to a $\tilde{G}$ and a photon. In such models there may still be events with only one photon detected, either because one photon is below threshold or not in the central region, or because of imperfect detection efficiencies. A lepton is a good signature for a chargino or vector boson decay from a cascade decay chain, and hence the $\ell\gamma\not\!\!E_t$ signature is again a signature of interest.

In gauge-mediated models if the gravitino is very light its lifetime can be long-enough so that sparticles can appear stable in the CDF detector[9]. In this case one would be more likely to detect only one photon, and, in the case where the stable particle was charged, a penetrating high-momentum particle that would be classified as a muon. The resulting signature would be a photon, 'muon', and $\not\!\!E_t + X$.

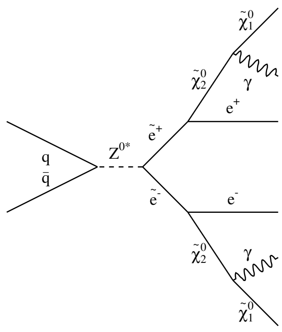

Figure 1: The Feynman diagram for $\tilde{e}$ pair production and decay in the $\tilde{\chi}_2^0 \rightarrow \gamma\tilde{\chi}_1^0$ scenario of Kane *et al.* Both selectrons decay via $\tilde{e} \rightarrow e\tilde{\chi}_2^0$ where $\tilde{\chi}_2^0$ is the next-to- lightest neutralino which in turn decays via $\tilde{\chi}_2^0 \rightarrow \gamma\tilde{\chi}_1^0$.

Another source of single photon events could be from gauge-mediated models but with R-parity violation[10]. In this case, either only one sparticle could be produced, or one of the pair of sparticles could decay via an R-parity violating decay before producing a photon and gravitino.

1.3 VX Associated Pair Production

Lastly, the photon-lepton signature is generally a powerful search engine for decays of pairs of heavy particles in which one of the pair is a vector boson. For example, the $ee\gamma\gamma\not{E}_t$ signature could be produced by ZX production, where X is a new particle that decays into a pair of charginos or sleptons (such as one of the Higgs bosons, for example). If the Z decays to $\nu\bar{\nu}$, one would expect the $ee\gamma\gamma$ system to be measured as recoiling against missing $\mathrm{E_T}$, as observed. In this case one might expect other events involving the other vector bosons, the W and the photon, as well as other decay modes of either the X or the boson[1] The photon-lepton signature for an inclusive search is ideal in that (as the reader will see below) it is highly selective, with only about one event per inverse picobarn passing the selection criteria.

1.4 Organization: CDF4976 and CDF4977

In this note we deal with the the SM expectations data in the $e\gamma$ and $\mu\gamma$ signatures for the 86.3 pb^{-1} of Run IB data. The data are presented in CDFnote CDF4977[5]. The $\tau\gamma$ channel

[1]It is interesting that in the $\mu\mu\gamma\gamma jj$ event the dilepton-diphoton system is recoiling with a transverse momentum similar to that in the $ee\gamma\gamma\not{E}_t$ event, but in this case against a system of two jets with an invariant mass consistent with that of the W or possibly the Z. In both events $\mathrm{p_T^{\ell\ell\gamma\gamma}}$ is approximately 55 GeV. This is the signature expected from VX production, where V is a vector boson (W or Z), and X is a heavy new particle coupled to massive particles, such as a Higgs boson.

is dealt with separately elsewhere[11].

1.5 Description of the Signature

We search the inclusive electron and muon samples, which are triggered on the lepton, for a high-E_T lepton and high-E_T photon, each with $E_T > 25$ GeV. We reject events that have one-and-only-one photon and one-and-only-one electron which are back-to-back with each other within $\pm 30^\circ$. We also consider the subsample with $\not\!\!E_T > 25$ GeV as a subset of the analysis.

Some changes from the previous analysis described in CDF3555 and CDF3851 are:

- The requirement of $\not\!\!E_T > 25$ GeV has been removed from the analysis: the signature is solely a high-E_T photon and a high-E_T muon or electron. The distributions in $\not\!\!E_t$ and the numbers of events both with and without significant $\not\!\!E_t$ are now compared to SM background predictions, rather than $\not\!\!E_t$ being a selection criterion early in the event selection chain.

- The central photon identification cuts now are the final cuts described in CDFnote 4580, and also include the Wilson corrections for lateral energy leakage[12, 13]. The cuts used are listed in Table 3. The main difference from the photon identification described in the gamma-gamma PRL and PRD is that we have removed the CES significance cut (it is not documented for Run Ib, and we believe that we can reject cosmic rays well with our other tools).

- The vertex used to calculate the photon E_T and the $\not\!\!E_t$ (and all other transverse energies) is the lepton vertex from the ELES or CMUO bank (*i.e.* the Class-10 or higher vertex closest in z to the z_0 of the lepton track), rather than the first vertex in the VTVZ bank.

2 Event Selection Criteria

2.1 Lepton and Photon Selection

The cuts used in this analysis, and in the selection of control samples for the estimate of Standard Model backgrounds, are shown in Table 2 for electrons and muons, and in Table 3 for global event variables and for photons. The code used in the final sample selection selection is given in Appendix A. The global event cuts are: a) requiring runs to be good runs (all systems working)[2], b) a good vertex, and c) no energy out-of-time. The photon is required to have $p_T > 25$ GeV and pass the tight photon cuts for photons that may come in on the box-isolation trigger (status code = 5000 [14]). A good electron must have $E_T > 25$ GeV and pass all TOPFND tight electron and isolation cuts (status code = 9000); while a good muon is one with $P_T > 25$ GeV/c which also passes all tight muon and isolation TOPFND cuts (status code= 7000). We emphasize that we have used TOPFND cuts for

[2]This is implemented as requiring BRCODE=31. We note that the top mass sample requires only BRCODE=15, and there are indeed some events in runs where the SVX is labelled as bad.

Inclusive Electron		
Central electron (ELES bank, type=0)		
E_T	$>$	18 GeV
P_T	$>$	13 GeV/c
HAD/EM (3 towers)	$<$	0.125
Lshr	$<$	0.2
χ^2(strip)	$<$	10
Track-CES matching:		
$* \ |\Delta z|$	$<$	5 cm
$* \ |\Delta x|$	$<$	3 cm
Inclusive Muon		
Central muon (CMUO bank)		
P_T	$>$	13 GeV/c
HAD energy	$<$	6 GeV (note: no cut on EM)
Track Stub Matching:		
$* \ |\Delta x|$	$<$	10 cm (CMU only and CMU-CMP)
$* \ |\Delta x|$	$<$	20 cm (CMP only)
$* \ |\Delta x|$	$<$	20 cm (CMX)

Table 1: Cuts used to strip the Inclusive Electron and Inclusive Muon data sample from the Run IB Stream A DSTs. The values are taken directly from ELES Banks, and momentum is not beam constrained.

the lepton selection and the (current) standard 'photon treaty' cuts for high-$\mathrm{p_T}$ photons, the latter being very close to those used for the published $\gamma\gamma$ analysis.

2.2 The Calculation of $\not\!\!E_{\mathrm{T}}$ selection for the LGAMMA Dataset

We use $\not\!\!E_{\mathrm{T}}$ corrected for muons, photons, electrons, and jets using the prescription of Toback[15]. The prescription is as follows. To correct for muons we take MET(4) from TOPFND. To correct for electrons and photons, we vectorially subtract from the $\not\!\!E_{\mathrm{T}}$ the uncorrected P_x and P_y from the associated ($\Delta R = 0.4$) JETS bank and add in the corrected (using CEMFIX or PEMFIX) electron or photon momentum. To correct for jets, we subtract the uncorrected momenta and add in the momenta corrected using JTC96S ('NN','DD') corrections. We note that all events have been revertexed using the electron or muon vertex, and the $\mathrm{E_T}$ of the jets, photons, and $\not\!\!E_{\mathrm{T}}$ have been recalculated with this vertex.

Inclusive Electron		
Central electron (ELES bank, type = 0)		
E_T	$>$	25 GeV
Fiducial cut		(FID_ELE = 0)
Conversion removal		(CON_WRD = 0)
E/p	$<$	1.8
HAD/EM (3 towers)	$<$	0.05
Lshr	$<$	0.2
χ^2(strip)	$<$	10
Track-CES matching:		
$*$ $\lvert\Delta z\rvert$	$<$	3 cm
$*$ $\lvert\Delta x\rvert$	$<$	1.5 cm
Track-Vertex matching: $\lvert\Delta z\rvert$	$<$	5 cm
Isolation E_T	$<$	$0.1 \times E_T$
Inclusive Muon		
Central muon (CMUO bank)		
P_T	$>$	25 GeV/c
HAD energy	$<$	6 GeV
EM energy	$<$	2 GeV
HAD + EM energy	$>$	0.2 GeV
Track Stub Matching:		
$*$ $\lvert\Delta x\rvert$	$<$	2 cm (CMU only and CMU-CMP)
$*$ $\lvert\Delta x\rvert$	$<$	5 cm (CMP only)
$*$ $\lvert\Delta x\rvert$	$<$	5 cm (CMX)
Track-Vertex matching:		
$*$ $\lvert\Delta z\rvert$	$<$	5 cm
$*$ d_0	$<$	0.3 cm
Isolation E_T	$<$	$0.1 \times P_T$

Table 2: The 25 GeV kinematic thresholds and the TOPFND identification selection criteria used to identify electron and muon candidates.

Global Event Cuts		
Good Run (Code = 31)		
$\lvert z_{event} \rvert$	$<$	60.0 cm
$\mathrm{E_T}$(out-of-time)	$=$	0 GeV

Photon Identification and Isolation Cuts		
Central photon (ELES bank, type=0)		
Photon $\mathrm{E_T}$	$>$	25 GeV
3D tracks with $P_T > 1$ GeV	$=$	0
3D tracks with $P_T \leq 1$ GeV	$\leq$	1
HAD/EM	$<$	$0.055 + 0.00045 \times E^{\gamma}$
$\chi^2_{Avg} = \left(\frac{\chi^2_{Strip} + \chi^2_{Wire}}{2}\right)$	$<$	20.0
$\lvert X_{CES} \rvert$	$<$	21.0 cm
$\lvert \mathrm{Z_{CES}} \rvert$	$>$	14 cm
$\lvert \mathrm{Z_{CES}} \rvert$	$<$	217 cm
$\mathrm{E^{cluster}_{2nd\ strip\ or\ wire}}$	$<$	$2.39 + 0.01 \times E^{\gamma}$ GeV
Corrected Isolation $\mathrm{E^{Iso}_{cone}}$	$<$	2 GeV
$\mathrm{P_T}$ of tracks in a cone of 0.4	$<$	5.0 GeV

Table 3: Event and photon selection criteria. The global event cuts are listed in the upper section of the table; the photon selection cuts are listed in the lower section.

3 Standard Model Background Estimates

The dominant physics backgrounds to the lepton+photon signature are Z^0 boson, $W + \gamma$, and $Z^0 + \gamma$ production. The dominant fake background is W/Z^0 plus a jet misidentified as a photon (a 'fake' photon); the probabilities of faking a high-p_T central electron or muon are significantly lower.

Muons, however, have some unique backgrounds as they are identified through the tracking, and, unlike electrons, do not have the calorimeter to measure the energy. There are three well-known backgrounds that can cause the muon $\not\!\!E_T$ distribution to be different from that of electrons. One source is cosmic rays that traverse the CTC; one 'leg' of the cosmic ray track can be in time, while the other is far enough out-of-time so that the pattern recognition code misses it entirely. Another is $Z^0 \rightarrow \mu^+\mu^-$ decays, with a 'lost' muon (i.e. the muon track is missed in the CTC, either by being too far forward or backward, or due to pattern recognition and/or hardware problems). A lost muon produces missing transverse energy, albeit in the direction of the muon. Lastly, there may be Standard Model processes that can contribute to a difference between muon and electron production; the $V - A$ decay of pseudo-scalar mesons, for example, preferentially produces muons over electrons due to the helicity suppression for electrons.

We address each of these backgrounds in turn below, with special attention to processes that can cause an electron/muon difference. A summary of the SM background contributions to the lepton-photon and lepton-photon-$\not\!\!E_T$ signatures is given in Table 16, where we have classified the backgrounds as "Real lepton, Real photon" "Real lepton, Fake photon", and "Fake lepton, Real or Fake photon".

3.1 $W\gamma$ and $Z^0\gamma$

3.2 Fake Photons from W + Jet Events

The signature of a high-p_T lepton, $\not\!\!E_T$, and a photon can be faked by a W + jet(s) event in which a jet mimics a photon. The lepton and the $\not\!\!E_T$ are real in the case of this background. The 'fake rate' for jets faking photons has been extensively studied by the Diboson group for the $W\gamma$ and $Z\gamma$ analyses[16], and by Toback in the $\gamma\gamma + X$ analysis[1], among others.

We use the Run I $W^\pm \to e^\pm\nu$ and $W^\pm \to \mu^\pm\nu$ datasets, described below, and the fake rates from Ref. [1] and Ref. [16] to get the number of events expected from this source. The method is to count the number of jets that could fake a 25 GeV photon in events that would pass the lepton-$\not\!\!E_T$ selection criteria, and to multiply by the appropriate fake rate.

3.2.1 The $W^\pm \to e^\pm\nu$ Data Set

The rate for events with an electron, $\not\!\!E_T$, and at least one central jet with $E_T > 25$ GeV is taken directly from the Run 1 data. The dataset used is the $W^\pm \to e^\pm\nu$ dataset[18], which is a subset of the inclusive electron dataset on the Chicago disks[18]. The ntuple (STntuple format[14]) for this dataset was made with the same executable as the lepton-photon ntuple, and the electron selection is identical (pstat(1)>9025), and is described in Table 1. The missing E_T selection is also identical, being the requirement that the variable METC described in Section 2.2 be greater than 25 GeV.

The counting of events before applying the fake rate is given in Table 4. We have required a good electron with $E_T > 25$ GeV and corrected $\not\!\!E_T$ >25 GeV.

Selection Criterion	Events	Jets
$W^\pm \to e^\pm\nu$ Sample- no cuts	67178	N.A.
BRCODE = 31	63143	N.A.
$\vert VZEV\vert < 60.$ cm	63142	N.A.
ETOUT = 0	61238	N.A.
ESTAT(1)> 9025	52184	N.A.
METC > 25	45450	N.A.
Jets> 25 (not e_1)	N.A.	2564
$\vert\eta^{jet}\vert < 1.0$	N.A.	1707
Jet not btb with electron	N.A.	1041

Table 4: The number of events with a good electron with $E_T > 25$ GeV and corrected $\not\!\!E_T$ >25 GeV, and the number of jets, in the $W^\pm \to e^\pm\nu$ sample used to calculate the rate of jets faking photons in $W^\pm \to e^\pm\nu$ events. The number of central jets with $E_T > 25$ GeV, and the number of those that are not back-to-back (BTB) with the electron are given. The last line in the table gives the number of jets used in the fake-photon calculation.

3.2.2 Estimating the Number of $e + \not\!\!E_T$ + Fake Photon Events

Both the $e\gamma$ and $W^\pm \to e^\pm\nu$ datasets are subsets of the inclusive electron sample. The signature of a good electron with $E_T > 25$ GeV is already satisfied in the $W^\pm \to e^\pm\nu$ sample. Consequently, the number of electron + photon + $\not\!\!E_T$ events from $W^\pm \to e^\pm\nu$ + jet events is given by:

$$N_{Jet}^{\gamma} = N^{Jet} \times R_{Jet}^{\gamma} \tag{1}$$

where N^{Jet} is the number of central jets that could fake a photon and R_{Jet}^{γ} is the fake rate for a jet to fake a photon.

To find the number of jets that could fake a photon, we start with events from the $\mathrm{W}^{\pm} \rightarrow e^{\pm}\nu$ sample with an electron and missing-$\mathrm{E_T}$ passing the same cuts as in the lepton-photon selection. We then count the number of events , and the number of jets per event, that satisfy the same requirement as the photon, to wit: a) central ($|\eta^{det}| < 1.0$), and b) not back-to-back ($\Delta\phi^{e\gamma} < 150°$). In the 45,450 events passing the good-run, electron, and $\not{E}_{\mathrm{T}}$ cuts of the 67,178 events in the sample, there are 1707 central jets with $\mathrm{E_T} > 25$ GeV, of which 1041 are not back-to-back (this is the total number of jets, and not events: because the fake rate is small the contribution from events with each of two jets faking a photon is negligible.). These events form the sample of events which can fake a lepton + photon + $\not{E}_t$.

We then need to multiply the number of jets that are central and not back-to-back by the probability that a jet fakes a photon. This probability has been estimated in the $\gamma\gamma + X$ analysis from dijet events for photon cuts that are very close to those used here; the differences are that we use the photon leakage energy corrections and have removed the CES sigma cut. Neither of these should have a significant change on high-Pt photons from jets passing all the other photon cuts relative to real prompt photons. The gamma-gamma analysis[1] found a fake rate for jets of $\mathrm{E_T} > 25$ GeV to pass the photon cuts of:

$$R_{Jet}^{real+fake} = 1.3 \times 10^{-3}, \tag{2}$$

flat with $\mathrm{E_T}$ as best as could be determined.

This estimate includes real (direct) photons from the Compton production of photon+jet, and is consequently an overestimate as the process $W + \gamma$ where the photon is real is accounted for separately.

The $W\gamma$ group[16], has estimated that for the cuts used by the Photon Group, on which are cuts are based, the true fake rate is smaller than the total rate of jets passing the photon cuts by almost a factor of 8. They find that for photons with $\mathrm{E_T} > 19$ GeV the fake rate is

$$R_{Jet}^{\gamma} = (1.7 \pm 2.5) \times 10^{-4}. \tag{3}$$

A study in progress[17] using isolated charged tracks to estimate the probability of a jet fragmenting into an isolated π^{+} or π^{-} gives:

$$R_{Jet}^{\gamma} = (1.7 \pm 0.8) \times 10^{-4}. \tag{4}$$

For now we conservatively take $(3 \pm 2) \times 10^{-4}$ as our estimate of the probability for a jet to fake a 25 GeV photon. The upper limit at 1σ covers the range of the Wgamma group estimate, and as we are at higher momentum it should be in fact more pure (less fakes). This number will be refined as our studies progress, but the contribution is small.

Using this fake rate and the number of central jets, we get:

$$N_{Jet}^{\gamma} = (3 \pm 2) \times 10^{-4} \times 1041 = 0.3 \pm 0.2 \text{ events}. \tag{5}$$

In summary, the fake photon rate in the $e\gamma \not{E}_t$ sample from W+jet events is $0.3^{\pm}0.2$ events, where we have been somewhat conservative. We note that this background should be approximately the same for muon and electron events (*i.e.* approximately proportional to the number of $W^{\pm} \rightarrow e^{\pm}\nu$ and $W^{\pm} \rightarrow \mu^{\pm}\nu$ events), as it is the photon that is fake.

3.2.3 Estimating the Number of $e+$ Fake Photon Events

While most of the W+jet events will have $\not{E}_T > 25$ GeV, some fraction will not, and so will contribute to the total $e\gamma$ sample. We estimate this by finding the fraction of $W + jet$ events that have $\not{E}_T < 25$ GeV.

We use a Herwig MC sample[21] made with a $W+1$ jet matrix element: out of a total of 11,916 events that have an electron and $\not{E}_T$ satisfying the cuts there are 2046 with METC< 25 GeV, for a fraction of 17±0.3%. To check this, we have looked at the VECBOS W+2 jet MC samples used by the top group[22]: we find 23 ± 3 % for the $W^{\pm} \rightarrow e^{\pm}\nu$ sample and 28 ± 4 % for the $W^{\pm} \rightarrow \mu^{\pm}\nu$ sample. This is not unreasonable given that one Monte Carlo generates W+ 1 jet and the other W+2 jets. We will use 20±10% as a conservative estimate of the fraction of W events with $\not{E}_T < 20$ GeV. Applying this to the expected number of events with $\not{E}_T$ we calculate the total number of events (with $\not{E}_T$ and without):

$$N^{\gamma}_{Jet} = (1.0/0.8) \times (0.3 \pm 0.2) \text{ events} = 0.4 \pm 0.3 \text{ events}. \tag{6}$$

3.2.4 The $W^{\pm} \rightarrow \mu^{\pm}\nu$ Data Set

The rate for events with a muon, $\not{E}_T$, and at least one central jet with $E_T > 25$ GeV is also taken directly from the Run 1 data. The $W^{\pm} \rightarrow \mu^{\pm}\nu$ dataset[18] is a subset of the inclusive muon dataset on the Chicago disks[18]. The muon selection from the Standard ntuple is identical to that of the lepton-photon sample. The missing E_T selection is also identical, METC > 25 GeV. The event selection is summarized in Table 1.

Selection Criterion	Events	Jets
$W^{\pm} \rightarrow \mu^{\pm}\nu$ Sample- no cuts	42872	N.A.
BRCODE = 31	40460	N.A.
$\|VZEV\| < 60.$ cm	40460	N.A.
ETOUT = 0	38811	N.A.
MUSTAT(1)> 7025	34090	N.A.
METC > 25	30119	N.A.
Jets> 25 (not μ_1)	N.A.	1648
$\|\eta^{jet}\| < 1.0$	N.A.	1054
Jet not btb with muon	N.A.	677

Table 5: The number of events with a good muon with $E_T > 25$ GeV and corrected $\not{E}_T$ >25 GeV, and the number of jets, in the $W^{\pm} \rightarrow \mu^{\pm}\nu$ sample used to calculate the rate of jets faking photons in $W^{\pm} \rightarrow \mu^{\pm}\nu$ events. The number of central jets with $E_T > 25$ GeV, and the number of those that are not back-to-back (BTB) with the muon are given.

3.2.5 Estimating the Number of $\mu + \not\!\!E_{\rm T}$ + Fake Photon Events

The number of muon + photon + $\not\!\!E_{\rm T}$ events from $\mathrm{W}^{\pm} \rightarrow e^{\pm}\nu$ + jet events is given by:

$$N_{Jet}^{\gamma} = N^{Jet} \times R_{Jet}^{\gamma} \tag{7}$$

where N^{Jet} is the number of central jets that could fake a photon and R_{Jet}^{γ} is the fake rate for a jet to fake a photon.

Using this fake rate and the number of central jets, we get:

$$N_{Jet}^{\gamma} = (3 \pm 2) \times 10^{-4} \times 677 = 0.2 \pm 0.1 \text{ events} \tag{8}$$

expected, including the real photons.

In summary, the fake photon contribution to the $\mu\gamma\not\!\!E_{\rm T}$ signature from W+jet events is 0.2 ± 0.1 events, where we have been somewhat conservative in the fake rate estimate.

3.2.6 Estimating the Number of μ+ Fake Photon Events

We use the same calculation as in the $\mathrm{W}^{\pm} \rightarrow e^{\pm}\nu$ case to find the total number of W+jet events from those that have $\not\!\!E_{\rm T} < 25$ GeV. Applying this to the expected number of events with $\not\!\!E_{\rm T}$ we calculate the total number of events (with $\not\!\!E_{\rm T}$ and without):

$$N_{Jet}^{\gamma} = (1.0/0.8) \times (0.2 \pm 0.1) \text{ events} = 0.3 \pm 0.2 \text{ events.} \tag{9}$$

3.3 Fake Photons from Z + Jet Events

3.3.1 The $\mathbf{Z}^0 \rightarrow e^+e^-$ Data Set

We use the ELEELE dataset[18], which is a subset of the inclusive electron dataset on the Chicago disks[18], being events with at least two ELE banks with loose isolation. The selection of the loose Z sample used to measure the fake photon rate from Z+jet events is described in Table 6.

3.3.2 Estimating the Number of e + Fake Photon Events

A Z event with a high-$\mathrm{E_T}$ central jet can fake the lepton-photon signature if the jet passes the photon cuts. We use the following strategy to estimate the number of such events.

1. We use the ELEELE sample with a good central electron (ESTAT(1)>9025) and a second ELES bank with ESTAT(2))>3020, 3015, or 3010 in the central, plug, or forward, respectively. We find 5694 events. We take this as the sum of the Z plus (high-mass) Drell-Yan.

2. Within these events, we find the number of central jets with $\mathrm{E_T} > 25$ GeV and not back-to-back with the electron. We find 105 jets.

3. We use the Pythia MC to get the fraction of events in all Z's produced with a central electron passing the same electron cuts as in the data. This fraction is $43 \pm 2\%$. We also find the fraction that also have a second electron with ESTAT(2))>3020, 3015, or 3010 in the central, plug, or forward, respectively. This fraction is $26 \pm 2\%$.

Selection Criterion	Events	Jets
$Z^0 \to e^+e^-$ Sample- no cuts	14131	N.A.
BRCODE = 31	13244	N.A.
$\|VZEV\| < 60.0$ cm	12598	N.A.
ETOUT = 0	12221	N.A.
ESTAT(1)> 9025	7476	N.A.
ESTAT(2)> 3020, 15 ,or 10	5694	N.A.
Jets> 25 (not e_1 or e_2)	N.A.	280
$\|\eta^{jet}\| < 1.0$	N.A.	188
Jet not btb with e_1	N.A.	105
ESTAT(1)> 9025	7476	N.A.
$\|M_{ee} - M_Z\| < 6$	5225	N.A.
EPT(2) > 0	2823	N.A.
EPT(2) > 10	2592	N.A.
EPT(2) > 25	2211	N.A.
Jets> 25 $\|\eta^{jet}\| < 1.0$	N.A.	178
Jet not btb with e_1	N.A.	116

Table 6: The numbers of events and or jets used in the fake-photon calculation for $Z^0 \to e^+e^-$ + jets faking the inclusive $e\gamma$+X signature. The numbers at the bottom of the table (below the line) are used in calculating the $Z^0 \to \mu^+\mu^-$ fake rates.

4. The 105 jets observed are from the sample that corresponds to the 26% of the total with both electrons identified. However, we are interested in the 43% that have an identified good central electron. We normalize the 105 jets up by the ratio of 43/26 to find the total number of central jets with $E_T > 25$ GeV in events with a good central electron from $Z^0 \to e^+e^-$ decay. This is 174 jets.

5. We multiply this number of jets by the fake rate per jet to get the number of fakes.

The statistical uncertainty is dominated by the statistics on the 105 central jets. The upper systematic uncertainty is dominated by the number of Z and Drell-Yan events accepted: to set an upper limit we take the number of events with a good first electron and *any* second ELES bank (7476 events), and scale up the 5694 events by this. The lower systematic is dominated by the Diboson group estimate that 90% of the fakes are in fact real photons. The final upper uncertainty is +30%; the lower uncertainty is -90%

The final answer then is:

$$N^{\gamma}_{Jet} = (43/26) \times 105 \times (1.3 \times 10^{-3}) = 0.23^{+0.07}_{-0.21} \text{ events} \tag{10}$$

As a check that we are not overestimating the contribution from background in the Z sample, we require the dielectron mass to be within 6 GeV of the Z mass and remove the ESTAT(2) cuts on the second electron. We see 5225 events and 116 central not-back-to-back jets, in the correct proportion, within the uncertainties.

3.3.3 Estimating the Number of $e + \not\!\!E_T$ + Fake Photon Events

A $Z^0 \to e^+e^-$ event with missing Et will be included in the $W^\pm \to e^\pm\nu$ sample, and so these events will already have been counted in the background estimate from $W^\pm \to e^\pm\nu$. However because of the difference between muons and electrons in Z decays in which one track is lost, it is worthwhile to calculate the size of the Z contribution independently.

In the $e\gamma \not\!\!E_T$ case there are two main contributions to the rate. First, in addition to having a jet fake a photon, we can lose an electron in the calorimeter to generate the missing Et. A second process is where the missing Et comes from mismeasurement of a jet or jets.

A *very* conservative upper limit on the number of second electrons that are lost can be set by postulating that every second electron that is non-fiducial is completely lost to the calorimeter and generates $\not\!\!E_T$ greater than 25 GeV. We find from the Monte Carlo that 27% of the second electrons in events with a good first electron are non-fiducial. The upper limit is then:

$$N^{\gamma}_{Jet} = 0.23^{+0.07}_{-0.21} \text{ events} \times 0.27 = 0.06^{+0.02}_{-0.06} \text{ events} \tag{11}$$

The second contribution can be obtained from the data itself. There are 11 events of the 105 with central not-back-to-back jets that also have $\not\!\!E_t > 25$ GeV. This gives a contribution of 0.02 ± 0.01 events.

For the final estimate we sum these two contributions to get

$$N^{\gamma}_{Jet} = 0.1 \pm 0.1 \tag{12}$$

events with a central electron, missing E_T, and a jet faking an electron, where we have been conservative (but it doesn't matter).

3.3.4 The $Z^0 \rightarrow \mu^+\mu^-$ Data Set

The dataset used is the $Z^0 \rightarrow \mu^+\mu^-$ dataset[18], which is a subset of the inclusive muon dataset on the Chicago disks[18]. The selection of the loose Z sample used to measure the fake photon rate from Z+jet events is described in Table 7.

Selection Criterion	Events	Central Jets $E_T > 25$
$Z^0 \rightarrow \mu^+\mu^-$ Sample- no cuts	6115	N.A.
BRCODE = 31	5749	N.A.
$\lvert VZEV \rvert < 60.$ cm	5749	N.A.
ETOUT = 0	5290	N.A.
MUSTAT(1)> 7025	4979	N.A.
MUPT(2)>20	4979	N.A.
Jets> 25 (not μ_1 or μ_2)	N.A.	291
$\lvert \eta^{jet} \rvert < 1.0$	N.A.	209
Jet not btb with μ_1	N.A.	117

Table 7: The numbers of events and or jets used in the fake-photon calculation for $Z^0 \rightarrow \mu^+\mu^-$ + jets faking the inclusive $\mu\gamma$+X signature.

3.3.5 Estimating the Number of μ + Fake Photon Events

As in the electron case, a $Z^0 \rightarrow \mu^+\mu^-$ event with $\not\!\!E_T$ will already have been counted in the background estimate from $W^{\pm} \rightarrow \mu^{\pm}\nu$. We calculate it here separately to see the size of the effect, as it is one place that muons and electrons can be quite different. To avoid double-counting we do not add it in separately to the total.

We use the same technique as for the electrons. There is, however, one fundamental difference between the two cases: when an electron is not identified there is (in general) no missing E_T, as the calorimeter still catches much or most of the electron's energy, while when a muon is not identified its transverse momentum is completely lost.

We proceed in two steps. First we find the contribution from events where both muons are identified: these will (in general) not have missing Et.

We use the $Z^0 \rightarrow \mu^+\mu^-$ sample to select events with one muon with MUSTAT>7025 and a second one with MUSTAT>2000 and $p_T > 10$ GeV. In addition we demand that the event have no out-of-time energy, have BRCODE=31 (all systems working, including the SVX), and $|Z_{vertex}| < 60$ cm. We find 209 central ($|\eta| < 1.0$) jets with $E_T > 25$ GeV. Of these 117 are not back-to-back with the first muon (taking only the first is conservative.) Using the fake-rate per 25 GeV central jet of 1.3×10^{-3} and the same treatment of uncertainties as in the electron case, we estimate

$$N^{\gamma}_{Jet} = 0.15^{+0.05}_{-0.13} \text{ events} \tag{13}$$

without $\not\!\!E_t$ from $Z^0 \rightarrow \mu^+\mu^-$ decays.

To calculate the total inclusive rate we need to calculate the (larger) number of events with $\not\!\!E_T$. This is calculated in the next section.

3.3.6 Estimating the Number of $\mu + \not\!\!E_T$ + Fake Photon Events

The strategy is as follows:

1. We use the $Z^0 \rightarrow e^+e^-$ sample, which is selected on the calorimeter identification of the electrons, to measure the fraction of $Z^0 \rightarrow e^+e^-$ events in which the CTC finds the track of the second electron (we require $p_T > 10$ GeV rather than 25 GeV to avoid worrying about large radiative effects, and rather than 0 to avoid accidentals.). Also we measure the tracking efficiency versus the rapidity of the second electron. (note: second-order corrections would take into account the different rapidity distributions of the first central electron or muon and the radiation from the leptons, but since the contribution is already included, and the corrections are expected to be small, we do not bother.).

2. Use the measured number of $Z^0 \rightarrow \mu^+\mu^-$ events in which both muons are found in the CTC and the ratio of missed/found from the electron case to predict the number of $Z^0 \rightarrow \mu^+\mu^-$ events with the second muon missed. Again, use $p_T > 10$ as the cut discriminating lost from found.

3. Use the $Z^0 \rightarrow e^+e^-$ sample to find the average number of central jets with $E_T > 25$ GeV *per event* in events in which the second electron has no track found ($p_T < 10$).

4. Multiply the average number of jets per event times the number of muon events with a 'lost' second muon to get the number of central jets in muon+missing Et events. This gives us the number where the lost muon has $p_T > 10$ GeV, and so is conservative, as

the requirement to fake the $\not{E}_T$ is 25 GeV. Figure 4b shows the distribution in E_T for $Z^0 \to e^+e^-$ events with a lost track.

5. Multiply by the fake rate to get the number of $\mu + `\gamma' + \not{E}_T$ events.

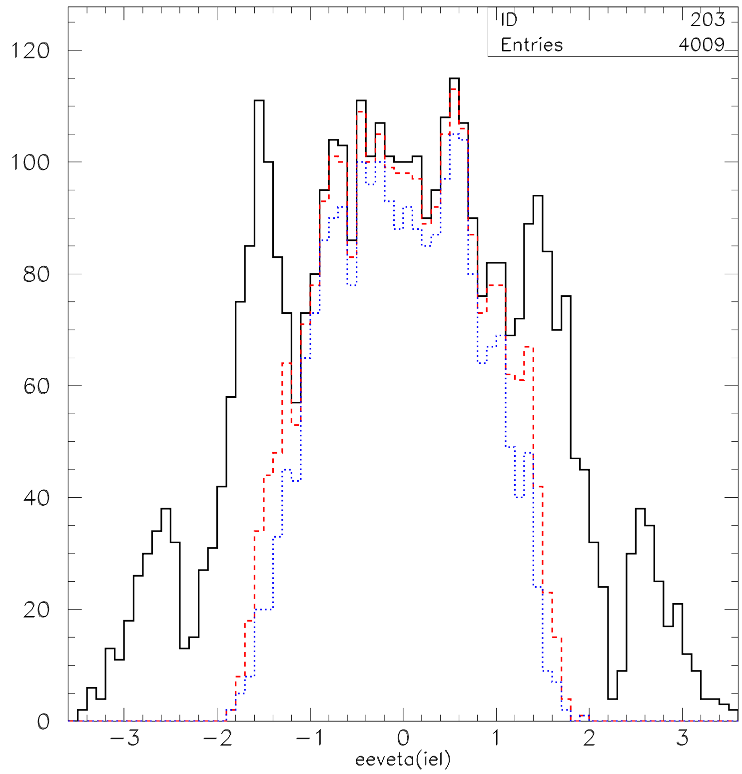

Figure 2: The rapidity distribution (event rapidity) of the second electron in events selected with a central electron with $E_T > 25$ GeV and a second ELES bank that makes an invariant mass within 6 GeV of the Z mass with the first, shown as the solid line. Also shown on the figure are the distributions for events in which the second electron has a track with $p_T > 10$ GeV (dashed line), and $p_T > 25$ GeV (dotted line).

Figure 2 shows the rapidity distribution (event rapidity) of the second electron in 5225 events selected with a central electron with $E_T > 25$ GeV and a second ELES bank that makes an invariant mass within 6 GeV of the Z mass with the first. Also shown on the figure is the distribution for events in which the second electron has a track with $p_T > 10$ GeV (EPT(2) > 10).

Figure 3 shows the ratio versus rapidity of the number of events in which the second electron has a track with $p_T > 10$ GeV to the total number events: this is, to first order, the track efficiency versus rapidity of the second electron. Also shown on the figure is the ratio of events in which the second electron does not have a track with $p_T > 10$ GeV (the inefficiency).[3]

[3]We use a 10 GeV cutoff to get rid of accidental tracks: the numbers change by approximately 10%, for events with $p_T > 0$ GeV from events with $p_T > 10$ GeV. The direction is conservative.

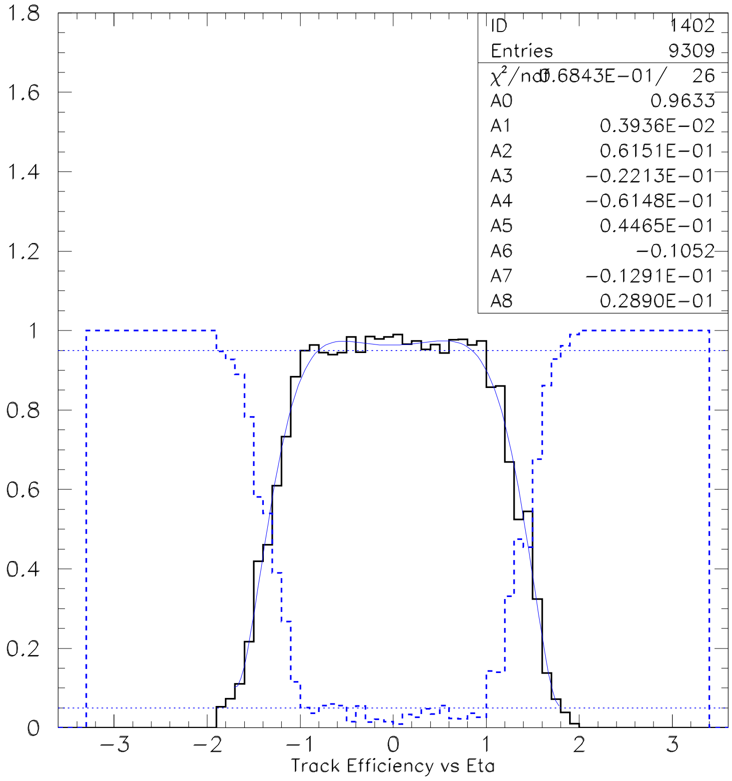

Figure 3: The ratio of events in which the second electron has a track to all events (the track efficiency) versus rapidity of the second electron (solid line). Also shown on the figure is the ratio of events in which the second electron does not have a track (the inefficiency–dashed line). Dotted lines are drawn at 95% and 5% efficiency to guide the eye. The fit is to an eighth-order polynomial. Note the EW asymmetry.

Figure 4a shows the distribution in p_T of the track of the second electron in events which have a track. Figure 4b shows the distribution in E_T of the second electron in events which do *not* have a track; this is the spectrum in $\not{E}_T$ for $Z^0 \to \mu^+\mu^-$ events in which one muon is lost. Also shown on this plot is the same spectrum for the subset of events which have a central jet with $E_T > 25$ GeV.

Out of the 5225 $Z^0 \to e^+e^-$ events, 2823 have a second electron with any track in the ELES bank (EPTZ0), 2592 have EPT$>$ 10 GeV, and 2211 have EPT$>$ 25 GeV. The respective fraction of $Z^0 \to e^+e^-$ events which have a second electron with a track (EPT > 0) is 0.54 ± 0.01. The fraction with a track with $p_T > 10$ GeV is 0.50 ± 0.01, and with $p_T > 25$ GeV is 0.42 ± 0.01. Using the 3384 $Z^0 \to \mu^+\mu^-$ events in which both muons are found we predict there are $(0.58/0.50) \times 3384 = 3925$ events with one muon with $p_T > 25$ GeV lost (and hence with missing $Et > 25$ GeV).

There are 76 central jets with $E_T > 25$ GeV in the 2633 events which have a second electron with no track with $p_T > 10$, giving an average number of 0.029 jets/event. We consequently expect 113 $Z^0 \to \mu^+\mu^-$ events with one muon with $E_T > 25$ GeV missing, and a central jet with $E_T > 25$ GeV, not back-to-back with the muon.

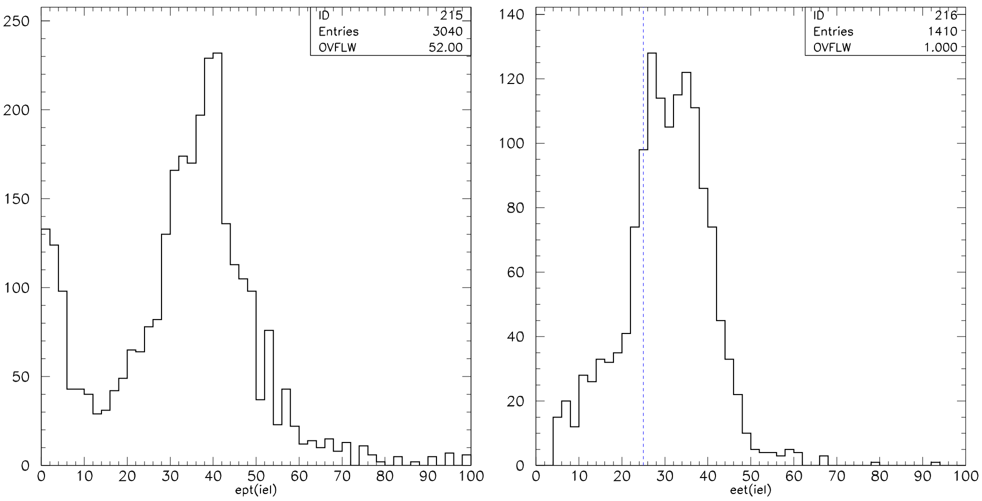

Figure 4: Left: the p_T spectrum for second electrons in $Z^0 \rightarrow e^+e^-$ events which have p_T greater than zero. Right: the E_T spectrum for second electrons in $Z^0 \rightarrow e^+e^-$ events which have PPT equal to zero. This spectrum should approximate the $\not\!\!E_T$ in $Z^0 \rightarrow \mu^+\mu^-$ events in which one muon is lost.

Finally, multiplying this number by the fake rate per 25 GeV central jet of 1.3×10^{-3} and the same treatment of uncertainties as in the electron case, we estimate

$$N^{\gamma}_{Jet} = 0.15^{+0.02}_{-0.13} \text{ events} \tag{14}$$

with $\not\!\!E_t$ from $Z^0 \rightarrow \mu^+\mu^-$ decays with a central jet faking the photon.

3.3.7 Comparison of the Tracking Efficiency versus Eta in QFL and Data

We have used the electron Z sample to measure the tracking efficiency versus rapidity (Figure 3). It is useful to see how well QFL reproduces the result. Figure 5 shows a comparison in $Z^0 \rightarrow e^+e^-$ events between the data (histogram) and Pythia (points) simulated by QFL.

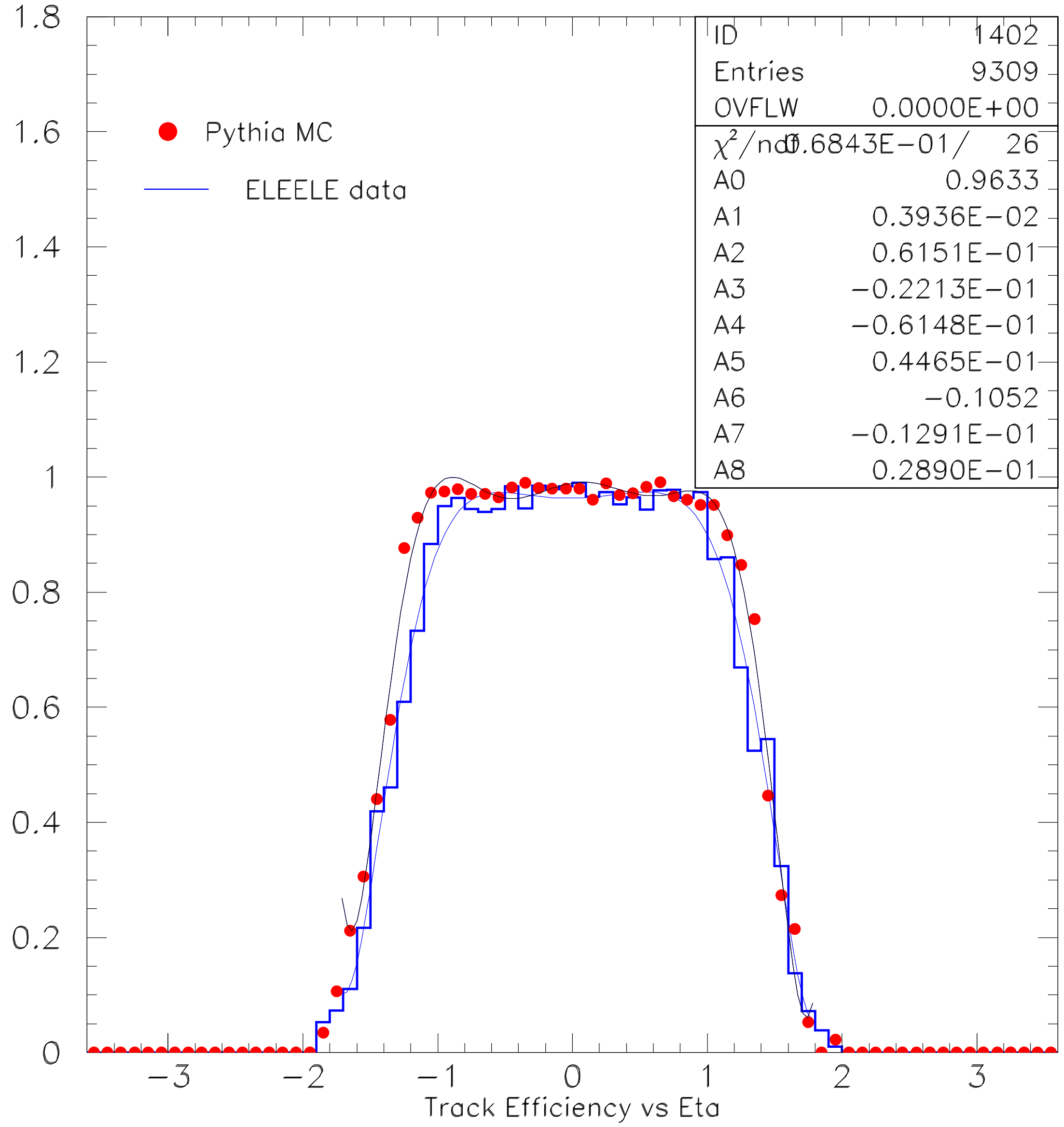

Figure 5: The ratio of events in which the second electron has a track to all events (the track efficiency) versus rapidity of the second electron from the $Z^0 \to e^+e^-$ data sample (histogram) and from Pythia simulated by QFL (points).

3.4 Cosmic Rays

Cosmic rays can produce isolated electromagnetic clusters that pass the photon cuts. These can be in conjunction with a muon that shows up as either one or two 'tracks' in the CTC, or, in the case that the muon penetrates the calorimeter tangentially, no track.

There are three cases to consider: 1) a real muon (from W-decay, for example) and an accidental cosmic-ray 'photon'; 2) a cosmic-ray muon and a real photon; and 3) a cosmic-ray muon and a correlated cosmic-ray photon, such as could possibly occur from multiple muons from an air-shower traversing the detector. We will consider the first case, a real-muon plus cosmic-photon, separately from the two cosmic-muon cases.

We have a number of handles on identifying cosmic rays in these events:

1. Timing of the electromagnetic calorimeter shower using the hadron calorimeter TDC's behind the photon cluster[23];
2. Impact parameter of the muon in an event with a muon.
3. The global sum of energy out-of-time in the hadron calorimeters;
4. CES/CPR alignment and CES pulseheight in photon showers;
5. Unattached muon 'stubs' in the muon chambers (stubs that do not have a track attached to them);
6. The hits left in the CTC back-to-back with a reconstructed single track.

3.4.1 Cosmic Ray Photon/Real muon

We use the hadron TDC timing of the photons for the quantitative estimate of this cosmic ray background; the other methods then are used as checks for consistency. Figure 6 shows the time distribution for the Z^0-like, Not-Z^0-like, and muon events. In all three cases about half of the events have a TDC hit in the hadron calorimeter, in good agreement with the fraction of 35% observed in electron showers from the W sample [24]. Defining the valid region as -20 to +35 nsec (this is the window used for the energy out-of-time sum) we observe zero events in each distribution outside the window.

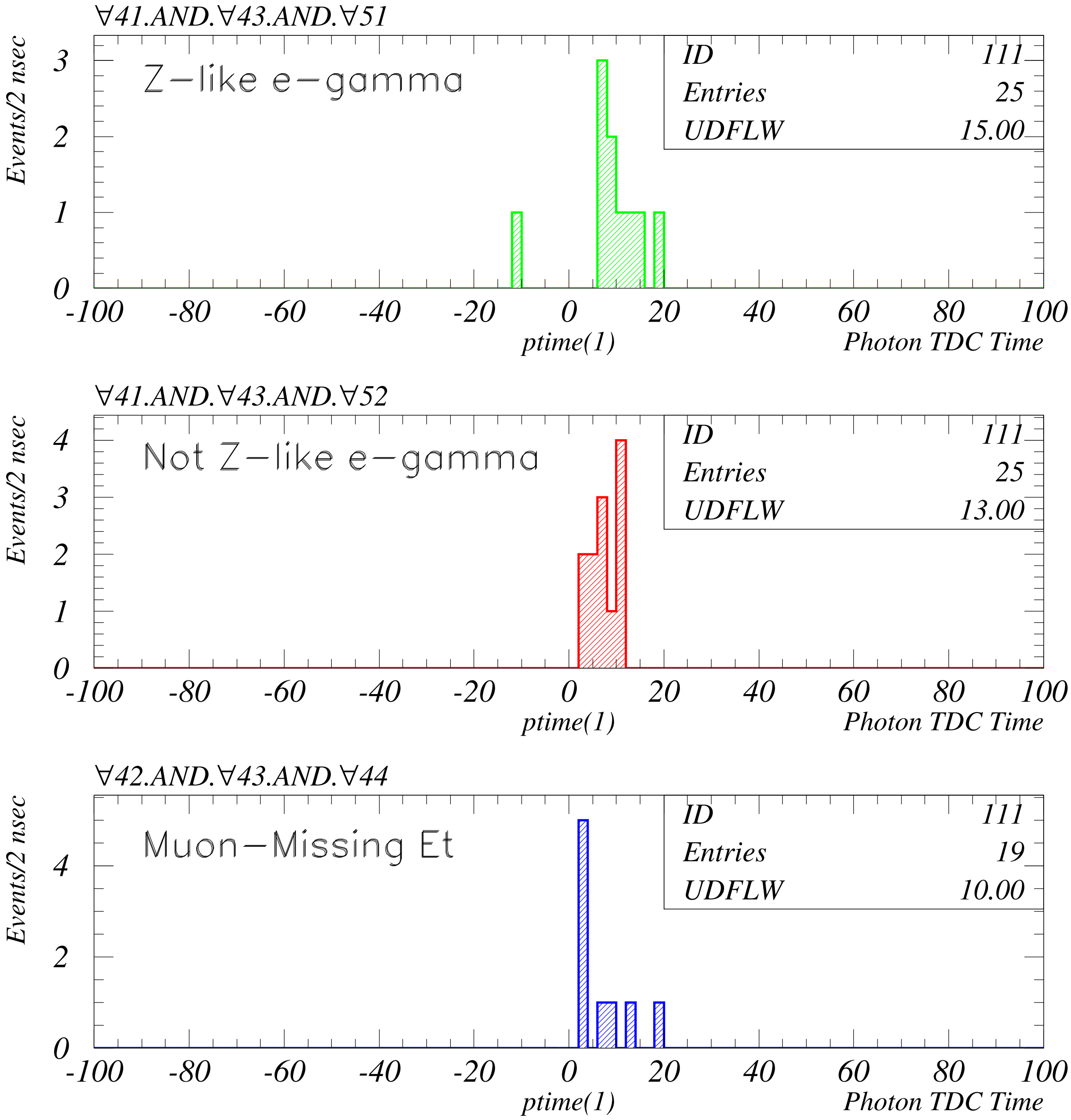

Figure 6: The hadron TDC time for the photons in Z^0-like (top), Not-Z^0-like (middle), and $\mu\gamma - \not{E}_t$ (bottom) events. Note the underflows (not all photons trigger the hadron TDC's.)

Cosmic rays should (and do) appear flat in time, assuming they are not correlated with the muon (or electron) observed in the event. We consider the uncorrelated case first. The time window for which the TDC is sensitive is from -100 to 580 nsec[25], so we can measure the number of events in the 625 nsec region outside the in-time window, and divide that by $625/55 \simeq 10$ to get the number of cosmic rays expected in the in-time window. We see zero events outside the in-time window in both the muon and electron samples. The central value for the expected number of cosmic ray photons in the muon sample is thus zero.

Using Poisson statistics, we set an upper limit at the 1 sigma level of 1.15 events expected in the out-of-time window (1.15 expected would give 0 observed with a 68.27% probability). The upper limit for in-time events for the sum of the electron and the muon samples is calculated as:

$$N^{68\%\mathrm{U.L.}}_{\mathrm{cosmicphotons}} = 1.15 \times 55/625 = 0.10 \text{ events.} \tag{15}$$

The muon sample alone should have half this value (the 0.1 event is the number for the sum of the electron and muon samples), as we expect the number of crossings with a real muon to be equal to that with a real electron (remember that we are calculating the number of 'accidental' cosmic photons with a real muon). We thus have a central value for the estimated background of 0.0, with a (one-sigma) upper limit of 0.05.

We emphasize that in this case, where we have assumed that the photon is uncorrelated with the lepton, that there should be the same number of cosmic ray background events in the electron and the muon samples. The excess of muon events, if due to cosmic rays, can only be because both the muon and the photon are due to a single cosmic ray event (possibly a shower either in the atmosphere or in the shielding above the detector), and hence the photon is 'in-time' by definition, as the timing of the event is determined by the muon.

3.4.2 Cosmic Ray Muon/Real or Cosmic Photon: the Cosmic Algorithm and the Data

A cosmic ray muon can accidentally land on top of a real photon event, or both the muon and the photon can be from one or more cosmic ray muons. However, in both cases the muon can be identified as a cosmic ray, so we treat these two cases as one. We can estimate the number of detected muons that are actually cosmic rays by looking at the muon TDC timing, the impact parameter distribution, and, most powerfully, by detecting the hits left by the particle back-to-back with the track found by the pattern recognition[4]

We use the cosmic ray muon sample of Andrew Scott [27], which is derived from $81.2pb^{-1}$ of Run IB dimuon data. We also have a $Z^0 \rightarrow \mu^+\mu^-$ sample created from the high-p_T inclusive muon sample with which to compare [28], as well as a $W^\pm \rightarrow \mu^\pm\nu$ sample to check the effect

[4] For new-comers, the CTC is built with sense-wire planes tilted with respect to a radial track so that high-p_T tracks cross the planes. Charge drifts in from each side of the plane so that in each superlayer there is one segment at larger radius and one at smaller radius to the point where the track crosses the plane. A Z decay, for example, can produce two muons which are both outward-going. A cosmic ray, however, produces 'two muons' one of which is in-going and the other which is out-going. The CTC pattern recognition code often will miss one or the other of these two 'tracks', as the separation of the two segments in each superlayer can be too large. However the hits are there, and can be reconstructed under the hypothesis that the track is going the 'wrong' direction.

on single track events.. We consequently can calibrate the separation between cosmic and real muons. We have developed the cosmic-muon algorithm independent of the lepton-gamma sample; it was applied to the signal sample only after the cuts were set. This is consequently a 'blind' test.

The algorithm is described in CDF note 4830 [24]. Briefly, it uses two discriminants: the time of the muon as measured by the hadron TDC, and the change in curvature of the track when the beam constraint is applied. $Z^0 \to \mu^+\mu^-$,$Z^0 \to e^+e^-$,$W^\pm \to e^\pm\nu$ and $W^\pm \to \mu^\pm\nu$ samples. The filter finds 80% of the one-legged cosmic rays while accepting $\sim 1\%$ of $Z^0 \to \mu^+\mu^-$ or $\sim 2\%$ of $W^\pm \to \mu^\pm\nu$ candidates.

Figure 7 shows the distributions in muon time from: a) the 17 events with a muon, photon, and $\not{E}_t$ from the lepton-photon sample; b) the $W^\pm \to \mu^\pm\nu$ sample, and c) the cosmic sample. Sixteen of the 17 lepton-photon events have a valid TDC; the remaining one is not-fiducial for the CMU, although it is fiducial for the CMP (this ratio is reasonable; 5.6% of the muons in the $Z^0 \to \mu^+\mu^-$ sample are non-fiducial. We thus expect 0.95 events and see 1).

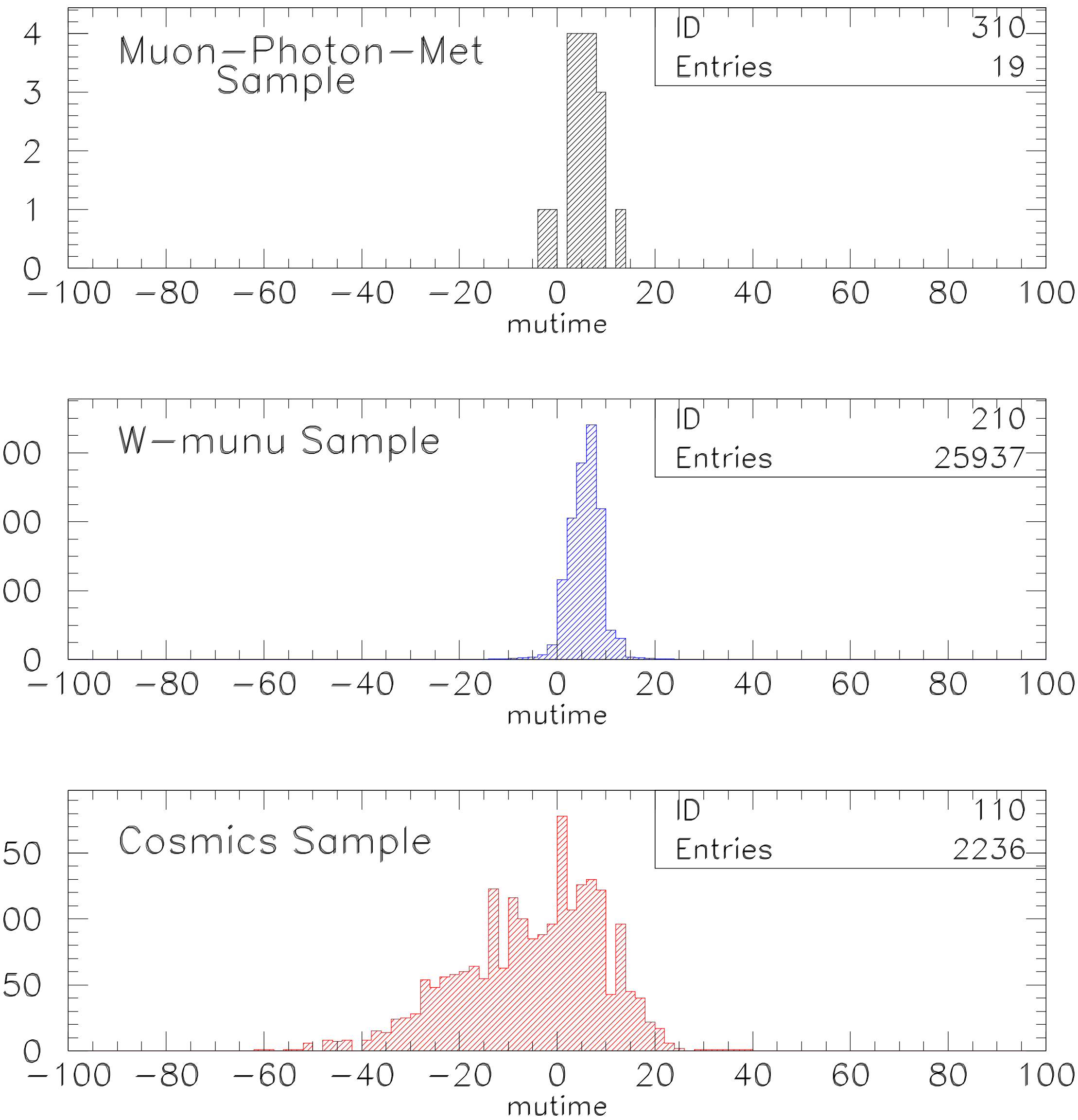

Figure 7: The hadron TDC time for muons in:a) the 17 events with a muon, photon, and $\not\!\!E_t$ from the lepton-photon sample; b) the $W^{\pm} \rightarrow \mu^{\pm}\nu$ sample, and c) the cosmic sample.

The change in curvature of the muon track, $D_{curvature}$, is defined as $(\mathrm{p_T^{bc}} - \mathrm{p_T^{raw}})/(\mathrm{p_T^{raw}})^2$. This is $\delta(1/\mathrm{p_T})$ under beam constraint, and should be (approximately) Gaussian. Figure 8 shows the distributions in the change in curvature of the muon track when beam-constrained for muons from: a) the 17 events with a muon, photon, and $\not{E}_t$ from the lepton-photon sample; b) the $\mathrm{W}^{\pm} \rightarrow \mu^{\pm}\nu$ sample, and c) the cosmic sample. All of the 17 lepton-photon events have a valid beam-constraint (i.e. the fit converged), and pass the *a priori* beam constraint cut. In contrast, 40% of the muons in the cosmic sample have tracks in which the beam constraint fails entirely. The cut was set on the Z sample to be highly efficient for muons from the Z while identifying a large fraction (80%) of cosmic rays. The cut value chosen (before looking at the lepton-photon sample distribution) was:

$$|(\mathrm{p_T^{bc}} - \mathrm{p_T^{raw}})/(\mathrm{p_T^{raw}})^2| < 0.015 \tag{16}$$

Of the 17 events in the lepton-photon sample, all 17 pass the delta-curvature cut. Sixteen of the 17 pass the cosmic filter described in CDF4830; the one event that fails is the non-CMU-fiducial event that has no TDC time. We conclude that the central value for the number of cosmic rays in the 17 events in the muon-photon-$\not{E}_t$ sample is zero.

To calculate the upper 'error bar' on the number of cosmic rays, we use the efficiencies of the filter for cosmic rays (80%) and for $\mathrm{Z}^0 \rightarrow \mu^+\mu^-$ events (1%). We ask the question "what is the mean number of cosmic ray events in the 17 muon-photon-$\not{E}_t$ events such that there is a 31% chance $(1-\sigma)$ that we see zero?". We find that an expected number of 1.22 cosmic rays is the $1-\sigma$ limit.

Figure 8 shows the distributions in delta-curvature from: a) the 17 events with a muon, photon, and $\not{E}_t$ from the lepton-photon sample; b) the $\mathrm{W}^{\pm} \rightarrow \mu^{\pm}\nu$ sample, and c) the cosmic sample. Events in which the beam-constraint failed are assigned the value ± 0.023, where the sign is the sign of the charge of the track, in order to appear on the plot.

The lepton-photon sample has some characteristics of both the cosmic background and the $\mathrm{W}^{\pm} \rightarrow \mu^{\pm}\nu$ sample. It differs from the cosmic sample in that there are no failures of the beam constraint (where 6.8 would be expected if all 17 were cosmics), but it has four events on the wings of the distribution, although inside the cut value. The four events are listed in Table 8. Only two have $\not{E}_{\mathrm{T}}$, and only one is in the final sample (the most interesting of these events with $\not{E}_{\mathrm{T}}$ has a 140 GeV photon opposite a 75 GeV muon, which fails the back-to-back cut). The times are squarely inside the peak of the muon time distribution for all four events. We conclude that there is no indication that these are cosmic rays.

RUN	EVENT	MUTIME(1) (nsec)	DPTREL(1) $(GeV)^{-1}$	$\mathrm{p_T^{mu}}$ (GeV)	NPVERT	VZEV (cm)
63078	25391	8.70	-0.0050	38.48	5	13.7
69036	49611	3.86	-0.0106	71.63	5	18.2
69464	118013	5.57	0.0082	47.00	10	16.5
70019	166983	3.13	-0.0076	56.76	3	-8.0

Table 8: The run and event numbers of the events with |delta-curvature| > 0.005 in the muon-photon sample. We have also tabulated the muon momentum, the delta-curvature, the muon TDC time, the number of VTVZ banks, and the z-coordinate used in the reconstruction (the muon vertex). All of these pass the *a priori* cosmic ray cut. Only one of these is in the final muon-photon-$\not\!\!E_{\mathrm{T}}$ sample; two fail the met cut, and one (70019), which has a 140 GeV photon opposite a 75 GeV muon, fails the back-to-back cut. See CDF4976.

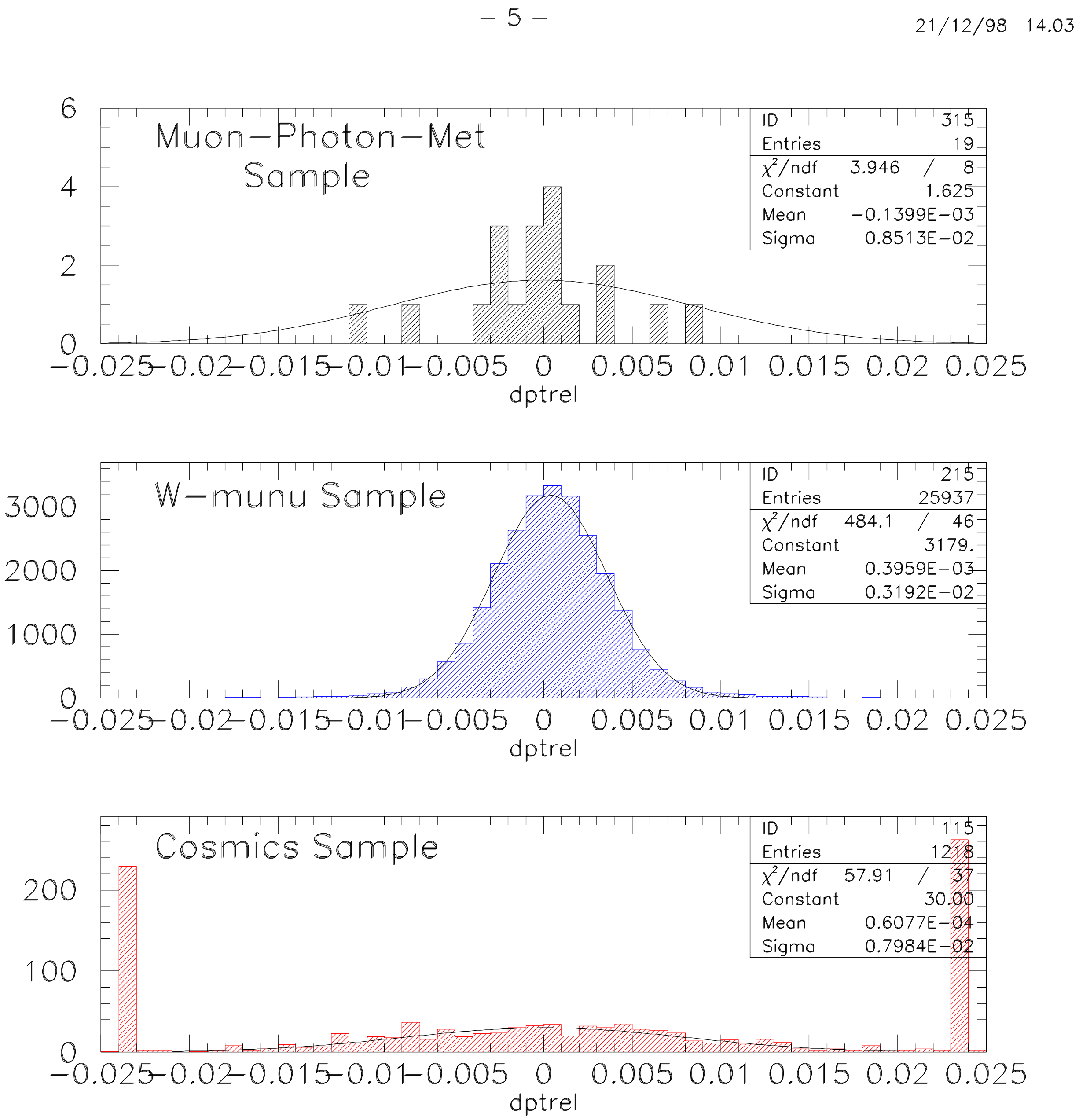

Figure 8: The change in curvature ($1/\mathrm{p_T}$) of the muon track in: the 19 events with a muon, photon, and $\not{E}_t$ from the lepton-photon sample; b) the $\mathrm{W}^{\pm} \to \mu^{\pm}\nu$ sample, and c) the cosmic sample.

3.4.3 Cosmic Ray Muon/Real or Cosmic Photon: an *a priori* Estimate

We can get an independent estimate of the expected number of cosmic ray events with a fake muon from the cosmic-ray sample and the $W^\pm \to \mu^\pm\nu$ samples as follows. We assume that the probability of getting a photon in a cosmic ray muon event is independent of whether or not the muon is 'one-legged' or 'two-legged'. The difference between the two samples is determined by the timing of the muon; as long as we require the photon to be away from the muon(s) and also not back-to-back with them (as we do), there should be no other difference.

We define the following variables:

$N_{1c} \equiv$ the number of one-legged cosmics
$N_{2c} \equiv$ the number of two-legged cosmics
$N_{1c}^{\gamma} \equiv$ the number of one-legged cosmics +photon
$N_{2c}^{\gamma} \equiv$ the number of two-legged cosmics +photon

Then our assumption is:

$$N_{1c}^{\gamma}/N_{1c} = N_{2c}^{\gamma}/N_{2c} \tag{17}$$

and so

$$N_{1c}^{\gamma} = N_{2c}^{\gamma} \times (N_{1c}/N_{2c}). \tag{18}$$

The number of one-legged cosmics, N_{1c}, is found from the $W^\pm \to \mu^\pm\nu$ sample [28] by selecting events that fail both the timing and delta-curvature cuts to be 61 events. The number of two-legged cosmics, N_{2c}, is found by selecting events that fail both the timing and delta-curvature cuts, from the cosmic sample (1165 events). Further requiring p_T^{muon} greater than 25 GeV (to be consistent with the 2-legged sample) reduces this number to 629 events [24]. The number of two-legged cosmics with a photon with E_T above 25 GeV is zero. Using a '1σ' expected number of 1.15 events for a 68% C.L., we thus expect $0.00^{+0.11}_{-0.00}$ events in which the muon is from cosmic rays. This is the estimate we use in the final summing of SM backgrounds.

3.5 Punchthrough

A muon can be faked by a hadron that either penetrates the calorimeter without an inelastic collision, or by one that interacts, but deposits less than 6 GeV in the hadron calorimeter and that also generates a muon stub with a good match to the track (this can be from a soft muon from the decay of a secondary in the interaction, or from a secondary hadron punching through). There have been several detailed studies of the probability of a specific hadron (π^+, π^-, K^+, K^-) punching through the calorimeter to the muon chambers[29, 30, 31, 32, 38, 39] using a number of techniques.

In order to estimate the number of muon events from hadrons faking muons, one needs to know the probability of a hadron punching through, and also the number of events that contain such a hadron and satisfy all the topological and kinematic requirements of the sample. To find how many candidates for punchthrough exist in the Run Ib data, we 'stripped' the Run Ib inclusive photon sample[26] of all events with a photon with $p_T > 25$ GeV that passes the cuts of Table 3 and also an isolated '3D'- track with $p_T > 20$ GeV. A total of 11,590 events[33] satisfied these criteria[5] , from an integrated luminosity of 87.4 pb^{-1}.

In the photon-lepton event analysis, muons are required to have $p_T > 25$ GeV. A total of 9138 events out of 11719 contain isolated tracks with $Pt > 25$ GeV/c. Most of these tracks have large values of η so they do not reach the outer layers of the CTC; the requirement for the track to have at least 3 axial and 2 stereo segments removes about 2/3 of them, leaving 2183 events. Also TOPFND, which is used to identify muons, requires the impact parameter to be small ($d_0 < 3$ mm). Adding these two requirements reduces the total number of events down to 1761, in which there are 873 positive tracks and 900 negative tracks. After requiring an event to have a photon passing all the cuts of the lepton-photon analysis, we are left with 904 events, of which 109 events have $\not{E}_T > 25$ GeV. Lastly, in order to eliminate Z decays where one loses a muon track but sees additional electromagnetic energy identified as a photon, we require that the azimuthal opening angle between the photon and the track be such that they are not back-to-back: $\Delta\phi < 150$ (degrees). This reduces the sample to 69 events with 38 positive and 33 negative high-Pt tracks. The criteria, and number of events which pass, for the photon-isolated track sample are summarized in Table 9. The distributions in the rapidity of the track, p_T of the track, impact parameter of the track, photon E_T, corrected missing E_T, and the delta-ϕ between the photon and the track, $\Delta\phi^{\gamma-track}$, are shown in Figure 9.

Requirement	Events	Tracks	Positives	Negatives
Inclusive Photon ($p_T^\gamma > 20$)	949,125	—-	—-	—-
Track with $p_T^{track} > 20$	11590	12041	5966	6041
$p_T^{track} > 25\ GeV/c$	9138	9352	4594	4758
Right number of segments	2183	2236	1106	1130
TOPFND isolation	2096	2111	1047	1064
$\|d0\| < 3mm$	1761	1773	873	900
Iso photon with $p_T^\gamma > 25$	904	914	446	468
$METC > 25GeV$	109	112	59	53
$\delta\phi(\gamma - track) < 150deg$	69	71	33	38

Table 9: The requirements for the selection of the photon + isolated-track sample, and the number of events tracks of each sign passing each cut. The corresponding integrated luminosity is 87.4 pb^{-1}. We use the 904 events before the $\not{E}_T$ cut to estimate the punchthrough before the back-to-back cut.

[5] Jeff stripped 11719 events. For some reason 129 of those do not have a high-Pt track in them.

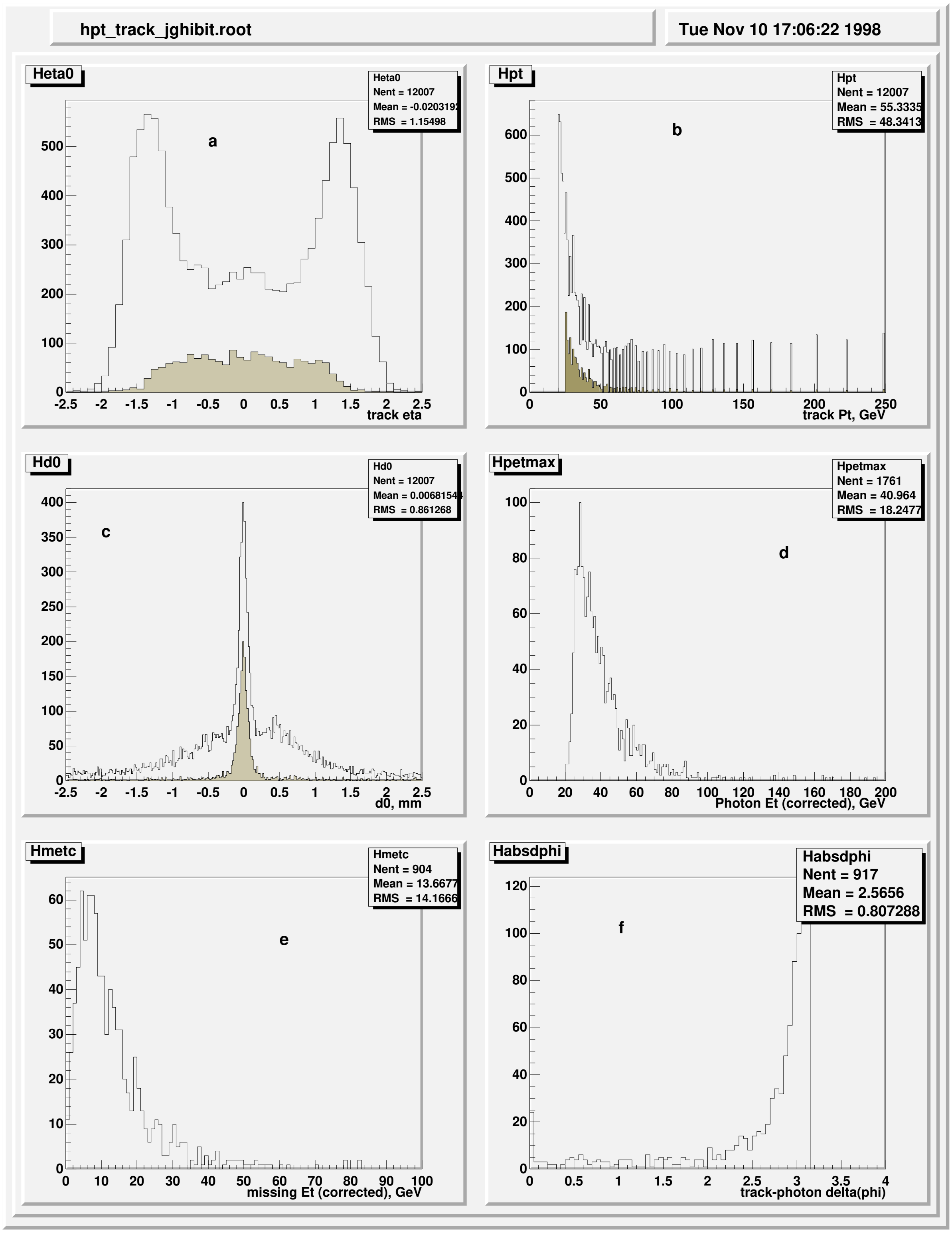

Figure 9: Distributions from the photon-isolated track sample in (reading from left to right, starting at the top): a) track η (before (light) and after (dark) track quality cuts), b) track $\mathrm{p_T}$, c) track impact parameter (before (light) and after (dark) track quality cuts), d) $\mathrm{E_T^\gamma}$ of the most energetic photon in the event e) corrected missing $\mathrm{E_T}$ (see Ref.[34] for the correction procedure) f) $\Delta\phi^{\gamma-track}$. The quantization in the $\mathrm{p_T^{track}}$ plot at large values of $\mathrm{p_T}$ is due to the finite resolution of the QTRK bank format.

To get an estimate of the size of the expected punchthrough, we use the program CMWINT, originally written by Dave Smith [29]. CMWINT computes the number of interaction lengths in depth for the calorimeter for high-momentum pions, K^+, and K^-. Table 10 gives the depth in absorbtion lengths for particles incident at 90° for the relevant range of momenta (there is very little variation at high momentum). We note that the thickness of the CDF calorimeter, typically 5 absorption lengths, corresponds to a hadron rejection factor of about 150[29].

Momentum (GeV)	Absorption Lengths (90 Degree Incidence)				
	K^+	K^-	$\pi^\pm$	p	$\bar{p}$
10	3.92	5.06	5.23	5.93	8.00
20	4.02	4.73	5.07	5.96	7.26
30	4.10	4.62	5.02	5.97	6.94
40	4.19	4.59	5.01	6.01	6.75
50	4.27	4.59	5.02	6.05	6.63
60	4.35 ± 0.20	4.60 ± 0.21	5.03 ± 0.23	6.09 ± 0.28	6.55 ± 0.29
100	4.54	4.64	5.07	6.18	6.39
150	4.59	4.57	5.05	6.11	6.36

Table 10: The number of interaction lengths (absorption lengths) for hadrons incident at 90° to reach the CMU. For a particle with polar angle θ, the number of interaction lengths increases by a factor of $1/\sin(\theta)$. Typical uncertainties are shown for 60 GeV (from Ref [29]).

We calculate the punchthrough using two different assumptions about the kaon fraction: 1) $K/\pi = 0.5$, motivated by high-p_T data at lower $\sqrt{s}$, and neutrino data[35], and, as a check of the worst case, 2), assuming all particles are kaons [36]. In both cases we assume there are no protons and anti-protons. This is conservative, as baryons and antibaryons have substantially larger interaction cross-sections than mesons, and so would contribute less to punchthrough. We start from the 904 events with 914 isolated tracks with $p_T > 25$ GeV in the gamma-track sample, of which 446 tracks are positive and 468 tracks are negative. For each track according to its sign we define a punchthrough probability

$$w \ = \ F_\pi \cdot exp(-\frac{\lambda_\pi}{\sin\theta}) \ + \ F_K \cdot exp(-\frac{\lambda_K}{\sin\theta})$$

where F_π and $F_K(F_{K^+} or F_{K^-})$ are the relative $\pi : K$ fractions (0.67:0.33 or 0:1) and λ_π and λ_K stand for the calorimeter thickness in units of the interaction lengths for the corresponding particle type; the punchthrough probability thus accounts for the differences in the cross-sections for different particle species.

The integral of the distribution for punchthrough probability gives an expected number of punchthrough hadrons. These numbers, calculated for different $\pi : K$ ratios, are presented in Table 11.

The procedure described above assumes the ideal calorimeter, and, for example, does not take into account the calorimeter cracks. As a check, we use inclusive high-Pt muon data[37] where we select muons that are in the fiducial region of *both* the CMU *and* the CMP, have

signature	total punchthrough	positive punchthrough	negative punchthrough
CMU ($\pi : K$=2:1)	3.5	2.0	1.5
CMU ($\pi : K$=0:1)	5.3	3.3	2.0
CMP ($\pi : K$=2:1)	0.2	0.12	0.08
CMP ($\pi : K$=0:1)	0.36	0.24	0.11

Table 11: Expected numbers of hadrons punching through the calorimeter up to the CMU (CMP) calculated with CMWINT for different $\pi : K$ ratios

$P_t > 25\ GeV/c$ and also pass the TOPFND muon identification and isolation cuts. The fraction of muons which have a segment in CMU but not in CMP allows an estimate of the punchthrough probability. The distribution for the muon detector code (segment bit pattern) is shown in Figure 10a. The code is: 0 = CMIO; 1 = CMU-segment only; 2 = CMP-segment only; and 3 = both CMU and CMP segments reconstructed. The sample contains 55 CMU-only, 23 CMP-only, and 1200 CMU-CMP muons. Figure 10.b shows their distribution in η.

CMU-only muons are either hadrons punching through the calorimeter or muons for which the CMP segment has not been reconstructed. To estimate the reconstruction efficiency in the CMP we use the $Z \rightarrow \mu\mu$ sample [42]. The distribution for the muon detector code for CMUP fiducial muons with $P_t > 25$ GeV/c which pass all the TOPFND cuts is presented in Figure 10.c. Considering events in the CMU-only bin to be due to the reconstruction inefficiencies in the CMP and to the multiple scattering between CMU and CMP (which we also include into the definition of inefficiency), we conclude that the reconstruction inefficiency in CMP is about $(3.0 \pm 0.2)\%$ Similarly the fraction of events in the CMP-only bin leads to the estimate of the segment reconstruction inefficiency in the CMU of $(4.0 \pm 0.3)\%$

We then count the number of isolated tracks in the inclusive muon sample that are not tagged as muons by either the CMU or CMP, and hence are likely to be hadrons (the *or* of the two systems should be efficient). There are 3298 isolated tracks with $P_t > 25$ GeV/c in this sample and which pass the selection cuts described on page 31 and have track $|\eta| < 0.6$ (we cut on track η to match the CMUP acceptance). Subtracting 1223 muon tracks leaves 2075 tracks which we assume to be hadrons. For a $\pi : K$ ratio of 2:1, the CMWINT-based procedure predicts that 14.2 hadrons will punch through the calorimeter. The CMP inefficiency accounts for $1223 \cdot 0.03 = 37$ CMU-only muons. Subtracting this number from 55 gives the expected number of punchthrough hadrons of 18 ± 9. This is consistent with CMWINT, however to be conservative we scale all the numbers obtained with CMWINT up by a factor of $18/14 = 1.3$.

Assuming $\not\!\!E_T$ to be uncorrelated with track p_T and the $\not\!\!E_T$ distribution for the punchthrough background in μ -photon data to be the same as for the photon-isolated track sample we repeat the calculations of the punchthrough probability described above for the photon-isolated track events with $\not\!\!E_T > 25$ GeV. The results are shown in Table 12. For a π/K ratio of 2:1 we expect 0.52 ± 0.25 “mu-gamma-met” background events (0.35 positive and 0.17 negative) from punchthrough before the $\Delta\phi < 2.5$ cut, and 0.3 ± 0.15 events (0.2 positive and 0.1 negative) after the cut.

signature	total punchthrough	positive punchthrough	negative punchthrough
CMU ($\pi : K$=2:1)	0.52	0.35	0.17
CMU ($\pi : K$=0:1)	0.78	0.52	0.26
CMP ($\pi : K$=2:1)	0.026	0.017	0.009
CMP ($\pi : K$=0:1)	0.052	0.039	0.013

Table 12: Expected numbers of hadrons punching through the calorimeter up to the CMU and CMP calculated with CMWINT for different $\pi : K$ ratios for events with $\not{E}_{\mathrm{T}} > 25 GeV$. The CMWINT numbers are scaled up by a factor of 1.3. No $\Delta\phi < 2.5$ cut is applied. The estimated uncertainty in all the numbers in the table is about 50%.

Finally, we return to the muon-photon sample to check the CMU/CMP patterns for the muon tracks. In Figure 10.e,f we show the distributions in muon detector code (reconstructed segment pattern) and η for all the muons with $P_t > 25$ GeV passing the TOPFND ID and isolation cuts and passing both the CMU and CMP fiducial cuts.

Ideally all the muons in Figure 10.e should have segments in both CMU and CMP. In the data there are *no* CMU-only muons; 20 out of 21 muons have both CMU and CMP segments. This is in good agreement with the CMWINT estimate (the one missing CMU segment is consistent with the estimate of CMU efficiencies presented above).

Momentum (GeV)	Absorption Lengths (90 Degree Incidence)				
	K^+	K^+	$\pi^\pm$	p	$\bar{p}$
10	6.18	8.03	8.28	9.35	12.74
20	6.34	7.49	8.02	9.41	11.50
30	6.48	7.30	7.93	9.44	10.97
40	6.61	7.25	7.92	9.49	10.67
50	6.74	7.25	7.92	9.56	10.48
60	6.86	7.27	7.95	9.62	10.35
100	7.17	7.33	8.01	9.76	10.10
150	7.25	7.22	7.97	9.66	10.04

Table 13: The number of interaction lengths (absorption lengths) for hadrons incident at 90° to reach the central muon upgrade, CMP as calculated by the routine CMWINT. For a particle with polar angle θ, the number of interaction lengths increases by a factor of $1/\sin(\theta)$.

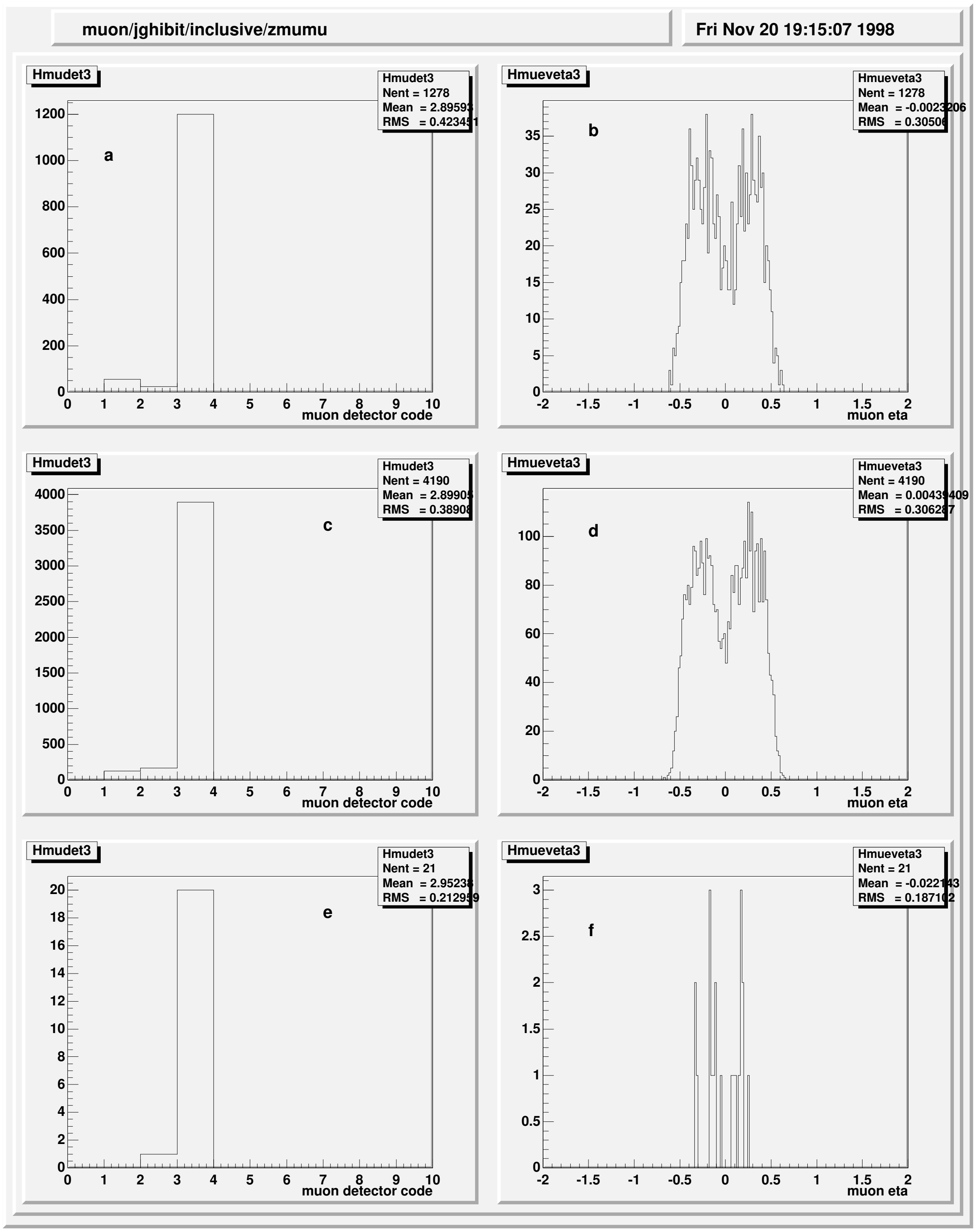

Figure 10: Distributions from the inclusive high-Pt muon sample for TOPFND muons with $P_t > 25GeV$: a) segment pattern for the reconstructed muon: 0 - CMIO 1 - CMU-only, 2 - CMP-only segment, 3 - both CMU and CMP segments reconstructed b) distribution in η for the muons in CMU-CMP fiducial c),d) - he same as a),b) but for $Z \to \mu\mu$ sample e),f) - he same as a),b) but for the photon-inclusive track sample

.

3.6 Decays-in-Flight

An estimate for the the number of fake $\mu\ \gamma\ \not{E}_{\mathrm{T}}$ events coming from pion and kaon decay in flight can be done in a similar way. To do this we conservatively assume that all the tracks have $\mathrm{p_T}\ =\ 25$ GeV/c. The probability for a 25 GeV pion to decay into $\mu\nu$ within 2 meters from the beampipe is about 0.15%. Kaons are heavier and have shorter lifetime so the probability for a 25 GeV kaon to decay into the same channel is about 4.5 times larger, i.e. about 0.68%. We also make another conservative assumption, namely that the cut on impact parameter for the muons from K/π semileptonic decays has the same efficiency as for the prompt muons.

Taking a $\pi : K$ ratio of $2 : 1$, we estimate the background from decays in flight to be less than 0.3 events. In the worst case, with all the secondary hadrons being kaons, the corresponding number is about 0.7 events.

3.7 Summary of punchthrough and decays in flight

In summary we estimate the background to $\mu\gamma\not{E}_{\mathrm{T}}$ channel from punchthrough at $0.5 \pm .25$ events and the background from the decays in flight to be less than 0.3 events, so the expected contribution from both background sources is less than 1 event.

3.8 $Z^0 \rightarrow \tau^+\tau^-$

The Z^0 boson can decay into τ^+ and τ^- where one τ subsequently decays leptonically and the other hadronically, the second decay chain leading to a final state containing at least one real photon. Here we estimate the background to the lepton+photon signature from events of this type, in which both the photon and the lepton come directly from decays of τ leptons.

Pythia 6.115 with the CTEQ4L parton distribution functions was used to generate $Z^0 \rightarrow \tau^+\tau^-$ events. Lowest order matrix element calculations were used. Amplitudes for the Z^0, Drell-Yan, and Z^0/Drell-Yan processes were included. Initial and final state radiation effects were enabled for QCD and QED processes. Daughter τ particles were redecayed by the TAUOLA program. The QFL detector simulation was run for the events generated by Pythia. The z-vertex distance for each event was sampled from Run IB data and lies between -60 cm and +60 cm. The only Pythia events which were kept are those for which $\sqrt{\hat{s}}$ of the parent partons was greater than 50 GeV. A total of 250,000 Monte Carlo $Z^0 \rightarrow \tau^+\tau^-$ events was generated, corresponding to a luminosity of about 1000 pb^{-1}.

It is useful at this stage to look at several plots showing various $\mathrm{E_T}$ and $\mathrm{p_T}$ distributions for these Monte Carlo events. For events containing at least one good photon, the corrected $\mathrm{p_T}$ value of the highest-status photon appears as the top plot in Figure 11. Likewise, a plot of the $\mathrm{E_T}$ distribution of the highest-status electron for events with at least one good electron appears as the middle plot. The bottom plot shows the $\mathrm{p_T}$ distribution of the highest-status muon in the events containing at least one good muon. All three plots in Figure 11 show distributions which cut off at 25 GeV (or GeV/c) because that is a requirement for a particle to be a good photon, electron, or muon. Also, we see that all the distributions exhibit a smooth decrease towards higher energies.

The top plot in Figure 12 shows the corrected missing transverse energy spectrum for the inclusive Monte Carlo sample of 250,000 events. The second figure shows the missing transverse energy in those events that pass all[6]. LGAMMA selection cuts listed in Appendix C. Notice that there are just four events that pass these cuts. In each of these events, the good lepton is an electron. Also, the corrected missing transverse energy values for these events are all less than 20 GeV. The third plot shows the value of $\Delta\phi$ between the good photon and the good electron in each of these events.

Only one event passes the requirement that $\Delta\phi$ be less than 150 degrees. The good photon in this event actually originated from a jet in final state radiation. This event would be included in an estimate of the background coming from $Z^0 \rightarrow \tau^+\tau^-$ + jet(s) processes, which is discussed separately in this paper. So this event is not included in the present estimate of the background coming from $Z^0 \rightarrow \tau^+\tau^-$ processes in which the photon comes from the decay of a hadronic daughter of the τ.

Therefore, in the 250,000 Monte Carlo events, there are no background events for the process $Z^0 \rightarrow \tau^+\tau^-$ in which the lepton comes from one τ and the photon comes from a hadronic decay product of the other τ. The error in the estimate of the background from this process may be found by comparing the luminosity of the Monte Carlo with the CDF Run IB luminosity: since the Z^0 cross-section times the branching ratio to $\tau^+\tau^-$ is about 240 inverse picobarns and 250,000 events were generated, the Monte Carlo luminosity is about 1042 inverse picobarns. Run IB luminosity is about 86.3 pb^{-1}, so the ratio between the Monte Carlo and real data luminosities is 11.7. This means that the error at 1σ is 0.15.

In summary, no event passes the missing $\mathrm{E_T}$ and the non-back-to-back requirements. The lepton+gamma background estimate for $Z^0 \rightarrow \tau^+\tau^-$ processes in which the lepton comes from one τ and the photon comes from a hadronic decay product of the other τ is $0.0^{+0.15}_{-0.0}$.

[6]The bad run code requirement is omitted since Monte Carlo data do not have bad run code values.

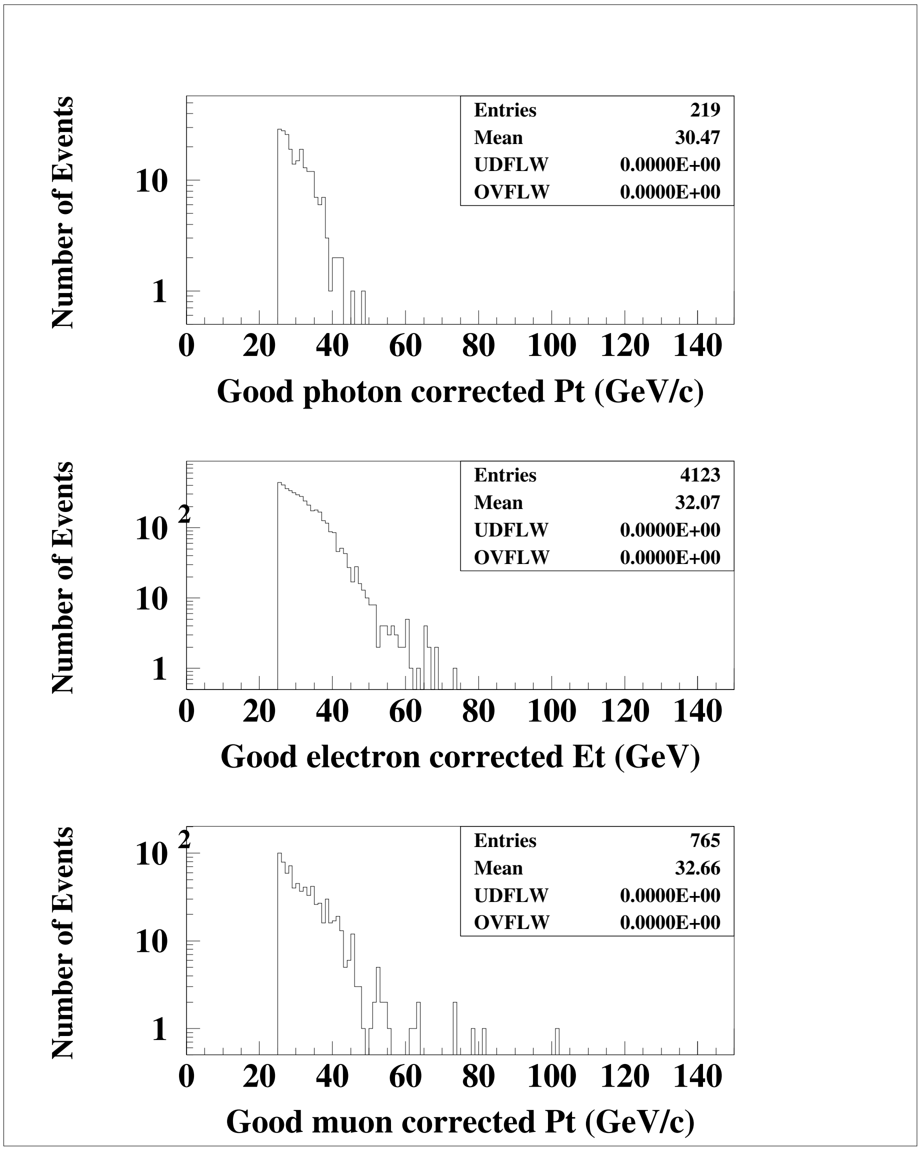

Figure 11: The p_T and E_T distributions for 'good' $Z^0 \to \tau^+\tau^-$ Monte Carlo events: (top) corrected p_T for the highest-status photon in events containing at least one good photon; (middle) corrected E_T for the highest-status electron in events with one or more good electrons; (bottom) corrected p_T for the highest-status muon in events with at least one good muon. The plots correspond to 1042 pb^{-1}.

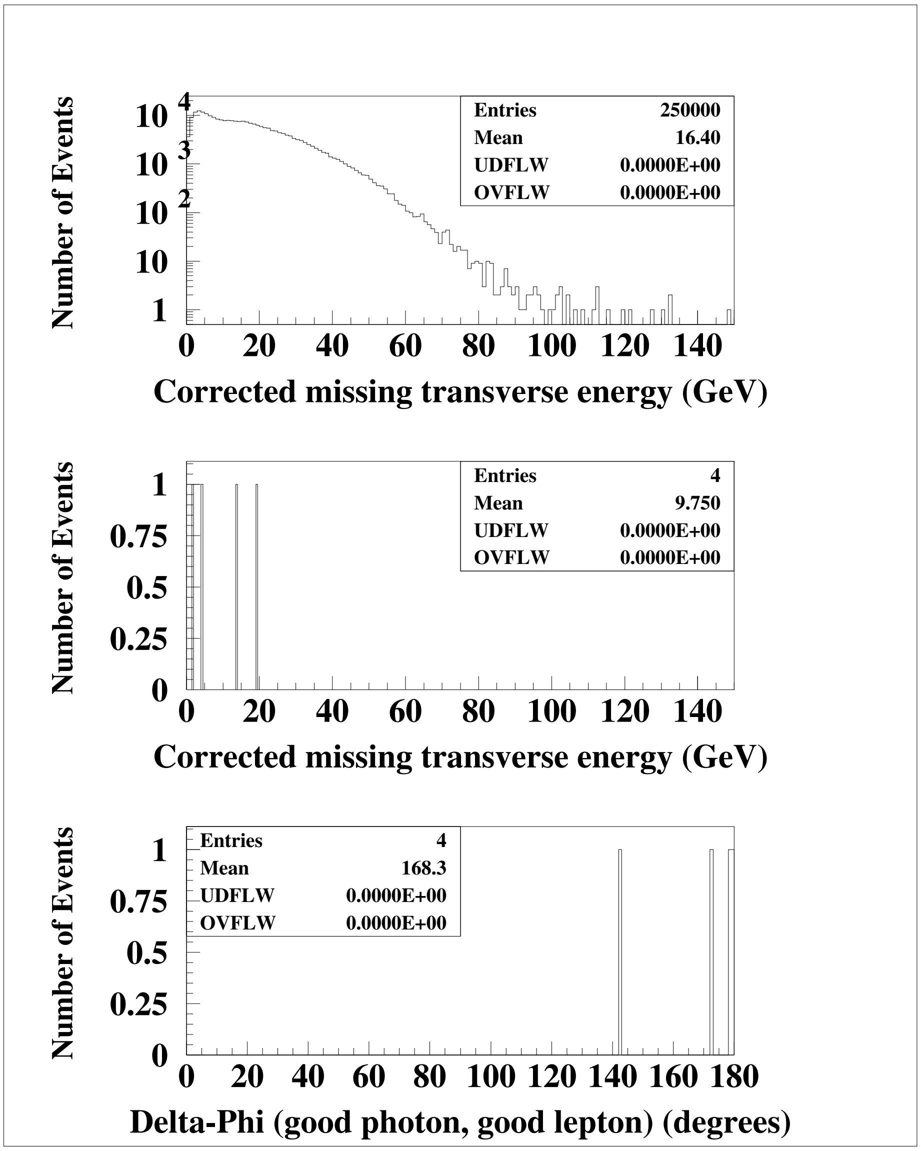

Figure 12: (top) Corrected missing transverse energy for the Monte Carlo $Z^0 \to \tau^+\tau^-$ sample; (middle) corrected missing transverse energy for the events passing the LGAMMA selection cuts; (bottom) the value of $\Delta\phi$ between the good photon and the good electron in the events passing the LGAMMA selection cuts.

3.9 Background from associative charm-photon production

Another source of background comes from the semileptonic decays of heavy quarks, in particular charm, produced in association with the photons. The dominant diagram for such a process is shown in Figure 13.

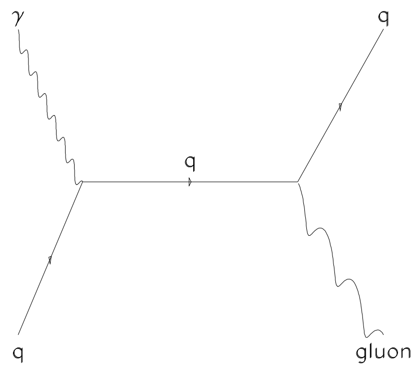

Figure 13: The Compton diagram that dominates heavy flavor production.

Charm-photon production has been extensively studied at CDF[38, 39] and from these studies one concludes that

- NLO QCD calculations describe the data CDF quite well
- the leading order calculations used in MC event generators (e.g. in Pythia) should be scaled up by a factor of about 2 to agree with the data.

We used Pythia 6.115 to generate heavy flavour-photon production and scaled the cross-section calculated by Pythia up by a factor of 2. As a cross-check we generated the Pythia charm-photon production process with the kinematic cuts described in Ref. [39], and obtained a cross section of 28 pb, to be compared with 26 pb from Ref. [39]. The details of the simulation are presented in Table 14.

A total of $3.2 \cdot 10^6$ events, corresponding to the integrated luminosity of 3.2 fb^{-1}, were generated. Events with photon $\mathrm{p_T} > 20$ GeV and lepton (electron or muon) $\mathrm{p_T} > 20$ GeV were simulated in the detector using the QFL$'$ simulation package. Three events, all e-gamma (no mu-gamma events) passed all the analysis cuts except the $\not\!\!E_t$cut. None of them passed the $\not\!\!E_t > 25$ GeV cut.

The corresponding estimated contributions to the inclusive $e+\gamma$ and $\mu+\gamma$ channels are $0^{+0.22}_{-0.0}$ events and $0.38^{+0.31}_{-0.2}$ events, respectively. The respective contributions to the $e\gamma\not\!\!E_{\mathrm{T}}$ and $\mu\gamma\not\!\!E_{\mathrm{T}}$ channels are $0^{+0.22}_{-0.0}$ and $0^{+0.22}_{-0.0}$ events.

3.10 Fake lepton+γ

There is a potential background in which the photon is real, but the lepton is fake, either in the sense that it is not a lepton at all, or that it is a lepton, but does not have $\mathrm{p_T} > 25$ GeV.

subprocesses	14, 29, 115
PDF function	CTEQ3L (4031)
Fragmentation model	Peterson: $\epsilon_c = 0.06$, $\epsilon_b = 0.0063$
Kinematical cuts	CKIN(3) = 20, CKIN(5) = 20
	CKIN(13) = -2.0, CKIN(14) = 2.0
	CKIN(15) = -2.0, CKIN(16) = 2.0

Table 14: PYTHIA settings used for the estimates of associative charm-photon production cross-section

The fake rate for tight central electrons with $p_T > 25$ GeV is negligible[1]; however, muons, for which the only measurement is with tracking, could be vulnerable. There are three 3 contributions to the fake muon + real photon rate, one of which we've already handled:

1. Punchthrough. This is already dealt with in Section 3.5.
2. Charm-gamma production via the Compton diagram. This background for real photons and real muons is estimated in Section 3.9. We consider here the rate for a soft muon being 'promoted' by non-Gaussian tails of the momentum resolution to satisfy the p_T cut. Note that the event has to pass the photon and $\not\!\!E_T$ criteria, and so the only contribution calculated here that is not already included in the gamma-charm estimate is due to the mismeasurement of the muon momenta by non-Gaussian tails.
3. Accidentals. There is the possibility that an isolated high-p_T hadron track points near a random stub in the muon system in an event that has a isolated high-E_T photon. A previous study[38] concluded that CMU-CMP accidentals are negligible, and but the accidental rate in the CMX predicted 12 ± 3 events with a muon above 4 GeV in 13 pb^{-1} in run Ia, for muons. For the present analysis, this will be greatly reduced by two large factors: 1) asking for a 25 GeV track rather than a 4 gev track; 2) the probability that the calorimeter sees less than 8 GeV if a 25 GeV track is incident on it in a fiducial region.

We deal with the latter two of these possible backgrounds in turn below:

3.10.1 Mismeasured muon momentum

To estimate the effect of non-Gaussian tails in the momentum resolution for muons we have convoluted the muon p_T-spectrum from

$$\bar{p}p \to \gamma c, \quad \text{followed by } c \to \mu + X \tag{19}$$

determined from Pythia, with a double Gaussian for the resolution determined by fitting the low edge of E/p (which is dominated by the upper tail in the momentum resolution) in the W mass analysis[40]. We then compare the number of events with $p_T > 25$ GeV with and without the wider tail in the resolution.

The fit to E/p in the W mass analysis[40] found that the lower side of the E/p distribution was well-described by a double-Gaussian with:

$$\sigma(1/pt) = 0.0009\ (1/GeV) \text{ for } 92\% \text{ of events} \tag{20}$$

and

$$\sigma(1/pt) = 0.026(1/GeV) \text{ for } 8\% \text{ of events} \tag{21}$$

A total of 1589 events was selected from the Monte Carlo with a cut on photon p_T of 25 GeV and on muon p_T of 5 GeV to get a representative low-p_T part of the spectrum. Then two spectra were generated:

- an "initial spectrum" – a histogram with 100000 random entries distributed according the distribution in muon p_T taken directly from the histogram;
- a "smeared spectrum" where each of the entries going into the "initial spectrum" was smeared with the double-Gaussian resolution.

The results are shown in Figure 14; the non-Gaussian tail has a negligible effect on the number of events above 25 GeV. As a cross-check, the distribution in delta(1/pt) between the smeared and non-smeared entries is also shown in Figure 14. We take zero as the contribution from this process.

3.10.2 Accidentals

Another way by which the detector signature of a muon can be faked is the presence of a spurious stub in the muon chambers in "accidental" coincidence with a hadron track pointing in that direction. If a non-muonic track is accidentally aligned with such a stub, there exists the possibility that the matched stub-track pair will pass the muon detection criteria. Spurious stubs are a problem largely in the CMX, where they arise from spray from the FEM calorimeter face and the face of the low-beta quads.
An estimate of the number of such events is obtained again from the photon/isolated track sample used in Section 3.5 Among the 104 events in this sample which have the same topology as the inclusive photon-lepton signal region, 53 have CMU-fiducial tracks, 54 have CMP-fiducial tracks, and 39 have CMX-fiducial tracks. An upper bound on the number of accidental matches for a particular muon detector type will be the number of detector-fiducial tracks (N_{track}) times the average density in ϕ of muon stubs ($\bar{n}_{\text{stub}}$) times the average target size in ϕ for a match ($\bar{\Phi}_{\text{match}}$):

$$N_{\text{match}} = N_{\text{track}} \times \bar{n}_{\text{stub}}(\text{rad/event}) \times \bar{\Phi}_{\text{match}} \tag{22}$$

The latter two numbers are determined by studying muon stubs in a sample of $Z \to e^+e^-$ events (ZEEFLT) [41] extracted from the inclusive electron sample (ICEFLT), which provides a uniform sampling of run conditions and a minimal contamination with real muons. Figures 15- 17 show the characteristics of CMU, CMP, and CMX stubs for these events. It is observed that the CMX is the dominant source of muon stubs.
The average target size in ϕ, $\bar{\Phi}_{\text{match}}$, is determined from the Δx cut for muons in Table 2, divided by the average cylindrical radius for a muon stub origin. The average stub density

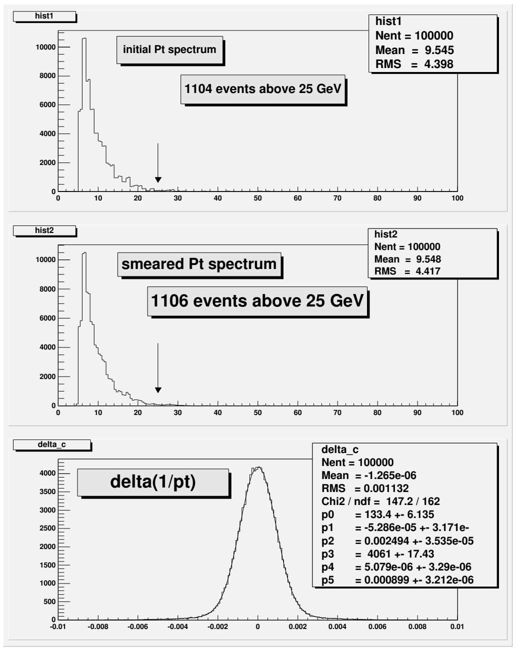

Figure 14: The effect of a wider component in the momentum resolution, as determined from fitting E/p in the W mass analysis, on the muon p_T spectrum in charm-photon production. The top plot shows the spectrum and number of events passing the 25 GeV cut for the normal spectrum; the middle plot shows the same after smearing with the double Gaussian. The bottom plot shows the effect of the smearing.

per radian per event $\bar{n}_{\text{stub}}$ is estimated by the total number of stubs found, divided by the total number of events, divided by the number of radians covered by the muon detector. Table 15 summarizes these results. It is determined that at most 0.2 photon-track events in Run IB could randomly match with a muon stub. Of those, only a small fraction will in turn pass the other muon selection criteria (particularly the calorimeter cuts), so that the total number of photon-fake muon events in our signal sample is negligible compared to other backgrounds.

Type	CMU	CMP	CMX
TOPFND Δx cut (cm)	2	5	5
Average radius (cm)	350	576	478
$\bar{\Phi}_{\text{match}}$	0.011	0.017	0.021
$\bar{n}_{\text{stub}}$	0.02	0.04	0.17
N_{track}	54	53	39
N_{match}	0.01	0.02	0.14

Table 15: Track-stub matching data for the ZEEFLT sample.

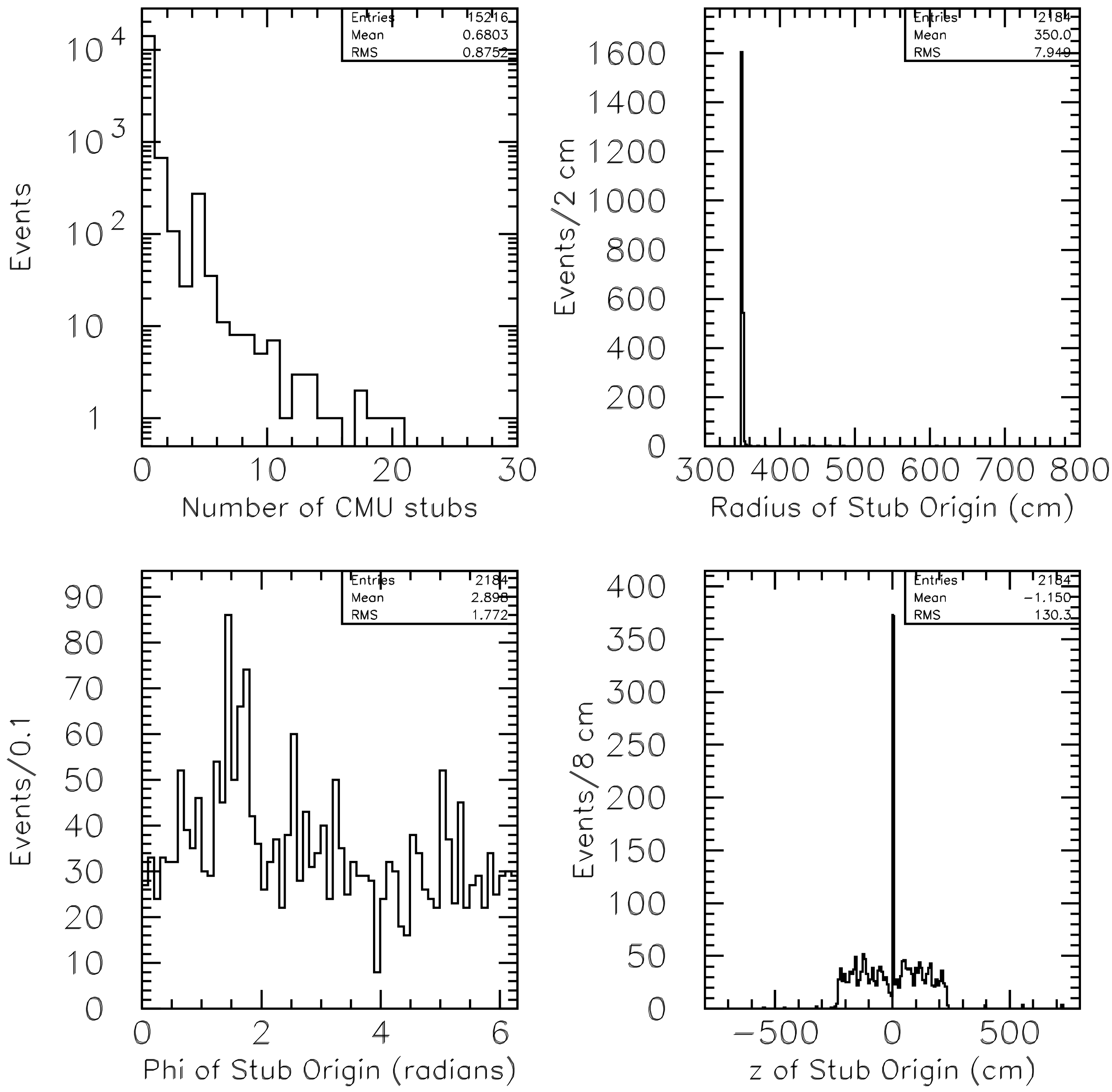

Figure 15: Clockwise from top left: For the ZEEFLT sample, the number of CMU stubs per event; the CMU stub origin r-coordinate; the CMU stub origin ϕ-coordinate; the CMU stub origin z-coordinate.

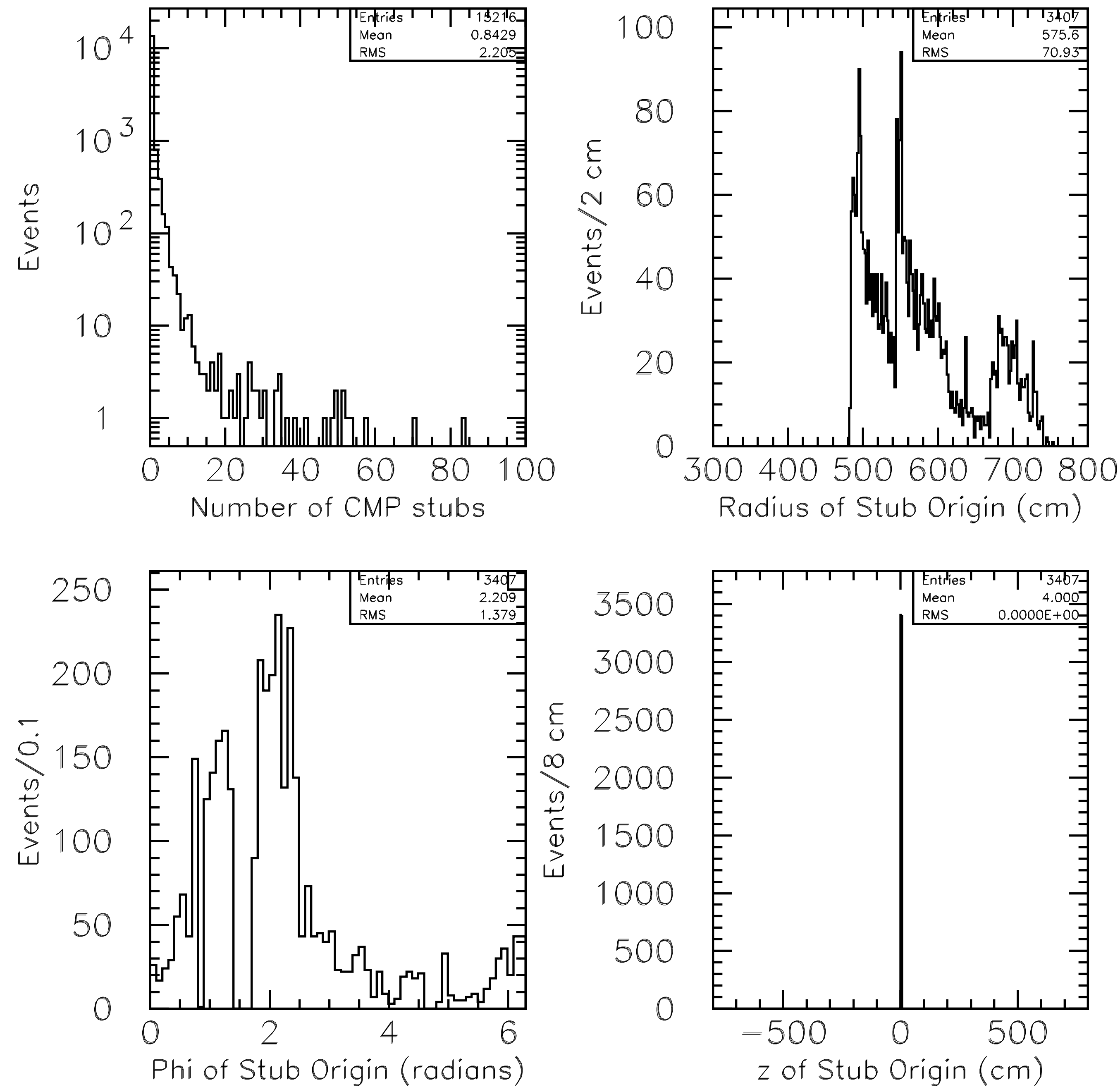

Figure 16: Clockwise from top left: For the ZEEFLT sample, the number of CMP stubs per event; the CMP stub origin r-coordinate; the CMP stub origin ϕ-coordinate; the CMP stub origin z-coordinate.

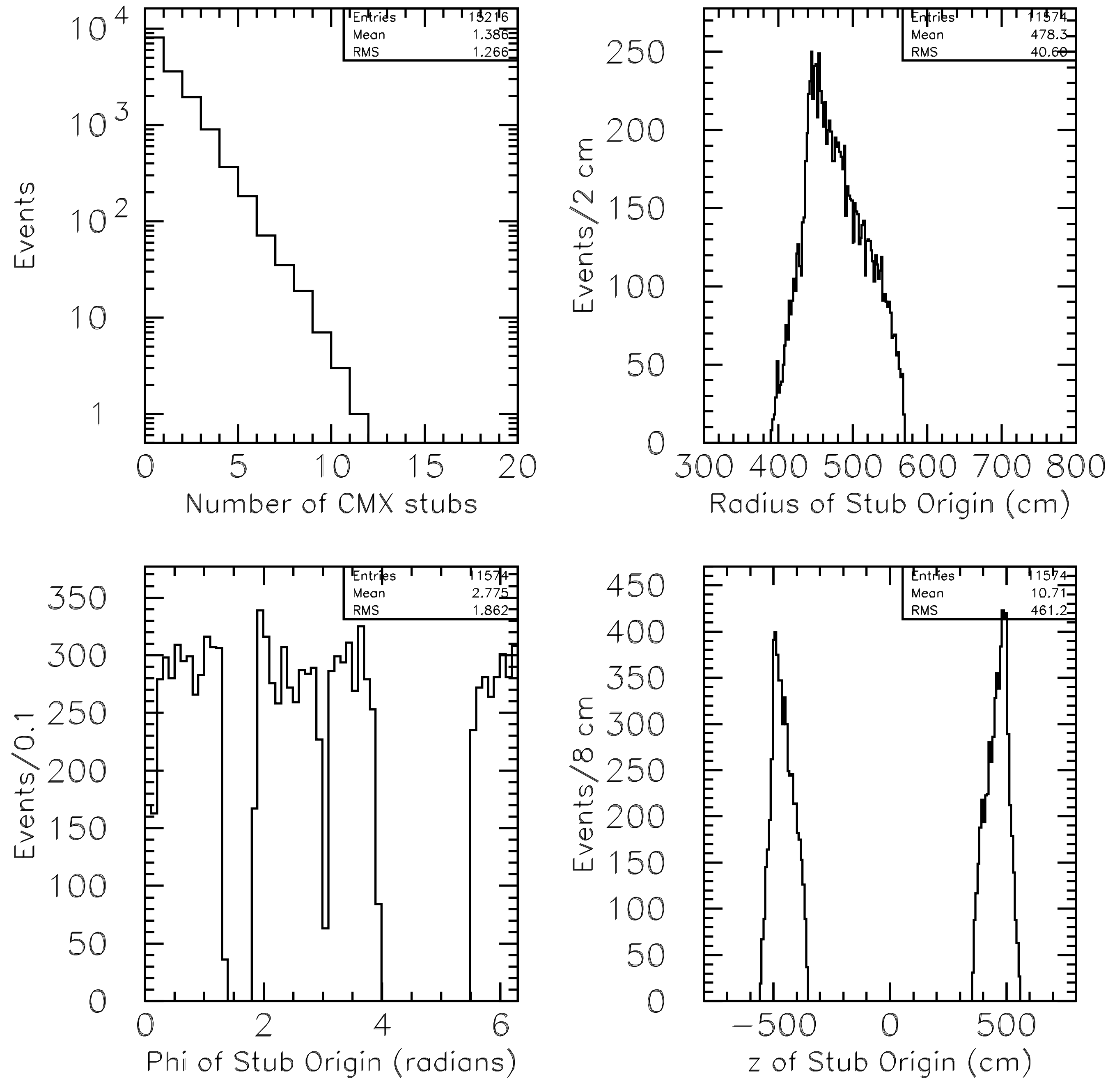

Figure 17: Clockwise from top left: For the ZEEFLT sample, the number of CMX stubs per event; the CMX stub origin r-coordinate; the CMX stub origin ϕ-coordinate; the CMX stub origin z-coordinate.

4 Totalling the Standard Model Backgrounds

Background Source	Electron+γ	Muon+γ	Electron+γ $\not\!\!E_T > 25$	Muon+γ $\not\!\!E_T > 25$
Real lepton, real photon				
W+γ	2.53 ± 0.31	2.39 ± 0.28	2.00 ± 0.26	1.83 ± 0.22
Z+γ	4.48 ± 0.41	4.17 ± 0.40	0.35 ± 0.05	0.97 ± 0.14
Real lepton, fake photon				
W+jet, jet $\rightarrow \gamma$	0.26 ± 0.26	0.17 ± 0.17	0.21 ± 0.21	0.14 ± 0.14
Z+jet, jet $\rightarrow \gamma$	0.03 ± 0.03	0.02 ± 0.02	(0.01 ± 0.01)	(0.02 ± 0.02)
$Z \rightarrow e^+e^-, e \rightarrow \gamma$	1.81 ± 0.45	N.A.	0.11 ± 0.05	N.A.
$Z \rightarrow \tau^+\tau^-, \tau \rightarrow e \rightarrow \gamma$	< 0.01	< 0.01	< 0.01	< 0.01
$Z \rightarrow \tau^+\tau^-, \tau \rightarrow \pi^0 \rightarrow \gamma$	$0.0^{+0.15}_{-0.0}$	$0.0^{+0.15}_{-0.0}$	$0.0^{+0.15}_{-0.0}$	$0.0^{+0.15}_{-0.0}$
Cosmic Ray γ	$0.0^{+0.05}_{-0.0}$	$0.0^{+0.05}_{-0.0}$	$0.0^{+0.05}_{-0.0}$	$0.0^{+0.05}_{-0.0}$
Fake lepton, real or fake photon				
Charm +γ	$0.38^{+0.31}_{-0.2}$	$0^{+0.22}_{-0.0}$	$0^{+0.22}_{-0.0}$	$0^{+0.22}_{-0.0}$
Cosmic Ray Muon	N.A.	$0.0^{+0.11}_{-0.0}$	N.A.	$0.0^{+0.11}_{-0.0}$
Punchthrough	N.A.	$0.69^{+0.37}_{-0.19}$	N.A.	$0.26^{+0.16}_{-0.07}$
π/K Decay	N.A.	$0.43^{+0.46}_{-0.23}$	N.A.	$0.15^{+0.16}_{-0.08}$
Fake Lepton+γ	N.A.	$0.0^{+0.1}_{-0.0}$	N.A.	$0.0^{+0.1}_{-0.0}$
Total Bkgd	$9.49^{+0.81}_{-0.76}$	$7.87^{+0.84}_{-0.60}$	$2.67^{+0.44}_{-0.34}$	$3.35^{+0.48}_{-0.31}$

Table 16: The estimated standard model backgrounds after the 'back-to-back cut' for the electron-photon and muon-photon samples. The estimates are shown with and without the missing E_T cut of $\not\!\!E_T > 25$ GeV. The notation N.A. means that this contribution has not been calculated, but is either not applicable, or is considered to be negligible. In some cases the background contains both a real lepton and a real photon, such as $W\gamma$ and $Z\gamma$ production. In others, such as W+jet or $Z^0 \rightarrow \tau^+\tau^-$, the photon is faked or produced secondarily. In yet others, such as punchthrough or cosmic rays, the lepton is faked.

The total backgrounds to each of the channels of $e - \gamma$ or $\mu - \gamma$ both with the $\not\!\!E_t$ requirement and without it are given in the next-to-last line of Table 16. The central value is just the sum of the individual backgrounds. The uncertainties are assumed to be uncorrelated.

5 Conclusions

We have estimated the contributions from Standard Model sources to the lepton-photon and lepton-photon-$\not\!\!E_T$ signatures. These expectations, shown in Table 16, are compared to the data in the companion CDF note, CDF4977[5].

6 Acknowledgments

We thank Uli Baur, Lina Galtieri, Lawrence Hall, Mark Lancaster, Tony Liss, Young-Kee Kim, Steve Mrenna, Hitoshi Murayama, Jon Rosner, David Toback, Peter Wilson, Weiming Yao for help along the way. We are especially grateful to Uli Baur and Steve Mrenna for their major efforts getting the $W\gamma$ and $Z^0\gamma$ theoretical and Monte Carlo situation in good shape.

7 Appendix A: The LGAMMA selection cuts

This is the COMIS file used to select the LGAMMA dataset from the CMUORELE_ELE dataset.

```
real function lgamma_filt(xdummy)

implicit none
include 'ghib$data:cwn.inc'
include 'c$inc:pivalu.inc'
integer xdummy
integer i,j,k
integer nele,ncmu,nphogood
real coriso

lgamma_filt = 0.0
nele = 0
ncmu = 0
nphogood = 0

do i = 1,nel
  if (estat(i).gt.9025) then
    nele = nele + 1
  endif
enddo

do i = 1,nmu
  if (mustat(i).gt.7025) then
    ncmu = ncmu + 1
  endif
enddo

do i = 1,npho
  if (pstat(i).gt.5000.and.petc(i).gt.25.0) then
    nphogood = nphogood + 1
  endif
enddo

if (etout.eq.0) then
if (brcode.ge.15) then
if (abs(vzev).lt.60.0) then
if (ncmu+nele.gt.0.and.nphogood.gt.0) then
  lgamma_filt = 1.0
endif
endif
```

```
endif
endif

return
end
```

References

[1] F. Abe et al., *Searches for New Physics in Diphoton Events in $\bar{p}p$ Collisions at Root(s)=1.8 TeV* , to be published in Phys. Rev. Lett., (hep- ex/9801019); F. Abe et al., *Searches for New Physics in Diphoton Events in $\bar{p}p$ Collisions at Root(s)=1.8 TeV* , submitted to Phys. Rev. D, June 1998 (hep- ex/9806034); D. Toback, Ph.D. thesis, University of Chicago, 1997.

[2] J. Berryhill, R. Culbertson, H. Frisch, and D. Toback, *A Search for SUSY Cousins of the $ee\gamma\gamma\not{E}_T$ Event in the $l\gamma\not{E}_T$ Channel*, CDF/ANAL/EXOTICS/3555, Feb. 1996.

[3] J. Berryhill, R. Culbertson, H. Frisch, D. Toback and P. Wilson *Update to CDFNote 3555: Search for Cousins of the eeggmet event in the $ell\gamma\not{E}_t$ Channel* CDF/ANAL/EXOTIC/CDFR/3851, Aug. 1996.

[4] R. Culbertson, H. Frisch, and D. Toback, *Search for Cousins of the $ee\gamma\gamma\not{E}_T$ Event In the Diphoton Channel*, CDF/ANAL/EXOTICS/3456, Dec. 1995.

[5] T. Andre, J. Berryhill, R.Culbertson, H.J. Frisch, N. Lai, P. Murat, and P. Wilson *Searching for Physics Beyond the Standard Model in the $e\gamma$ and $\mu\gamma$ Channels II: The Data*

[6] Haber, H. E., G. L. Kane, and M. Quiros, Phys. Lett. B **160**, 297; Haber, H. E., G. L. Kane, and M. Quiros, Nucl. Phys. B **273**, 333;

[7] S. Ambrosanio, G.L. Kane, G.D. Kribs, S.P. Martin, and S. Mrenna, Phys. Rev. Lett. **76**, 3498; S. Ambrosanio, G. L. Kane, G. D. Kribs, S. P. Martin, and S. Mrenna, Phys. Rev. D **54**, 5395.

[8] Dine, M., A. E. Nelson, and Y. Shirman, Phys. Rev. D **51**, 1362; Dine, M., A. E. Nelson, and Y. Shirman, Phys. Rev. D **53**, 2658; Dimopoulos, S., M. Dine, S. Raby, and S. Thomas, Phys. Rev. Lett. **76**, 3494; Dimopoulos, S., M. Dine, S. Raby, and S. Thomas, Phys. Rev. D **55**, 1372 (1997).

[9] M. Dine, W. Fischler, and M. Srednicki, Nucl. Phys. B189, 575 (1981); S. Dimopoulos and S. Raby, Nucl. Phys. B192, 353 (1981), and also M. Carena et al and references therein, below.

[10] See, for example, D.E. Kaplan, A. Nelson, *Solar and Atmospheric Neutrino Oscillations from Bilinear R-Parity Violation*, UW/99-02; hep-ph/9901254. See also M. Carena, S. Pokorski, and C.E.M. Wagner, *Photon Signatures for Low Energy Supersymmetry Breaking and Broken R-parity*, hep-ph/9801251.

[11] P.Murat, T.Andre, J.Berryhill, H.J. Frisch, *Search for Non-SM production in the Tau-Gamma Channel* CDF/ANAL/EXOTIC/CDFR/4702, Aug., 1998.

[12] Peter Wilson *Calorimeter Isolation and Lateral Shower Leakage for Photons and Electrons*, CDF/ANAL/EXOTIC/CDFR/4170, (rev.) 1/23/98

[13] H. Frisch and P. Wilson, *Search for Anomalous High Mass Diphoton Production* CDF/ANAL/EXOTIC/CDFR/4338, (rev.) 2/16/98

[14] This is the University of Chicago Standard Ntuple (STntuple) format: see http:hep.uchicago.edu for the definitions of the status codes and other variables. We are happy to share the executable and all tools with any interested CDF party.

[15] D. Toback, Ph.D. thesis, University of Chicago, 1997.

[16] B. Wagner, M. Lindgren, T. Muller, D. Neuberger, S. Errede, M Vondracek, and D. Benjamin, *Measurement of QCD Background in the $W\gamma/Z\gamma$ Analysis*, CDF2229; D. Benjamin, D. Errede, S. Errede, M. Lindgren, T. Muller, D. Neuberger, M. Timko, M. Vondracek, R.G. Wagner, *Measurement of $W\gamma$ and $Z\gamma$ Cross Sections in the Electron and Muon Channels with the 1992/1993 Data and Search for Anomalous $W\gamma$ and $Z\gamma$ Couplings*, CDF2430.

[17] J.G. Wacker, H.J. Frisch, and Y.K. Kim, analysis in progress; see $http://hep.uchicago.edu/cdf/gmet/gmet.html$.

[18] The $W^{\pm} \rightarrow e^{\pm}\nu$ and $W^{\pm} \rightarrow \mu^{\pm}\nu$ samples are described in $http://hep.uchicago.edu/cdf/ntuple\_datasets.html$.

[19] J. Berryhill, R. Culbertson, C. Grosso-Pilcher, P.J. Wilson, H.J. Frisch *Photon Selection for Exotic Analyses* CDF/ANAL/EXOTIC/CDFR/4580, 5/7/98.

[20] F. Abe et al, *Evidence for top quark production in $\bar{p}p$ collisions at $\sqrt{s} = 1.8$ TeV*, Phys. Rev. D50, 2966 (1994)

[21] L. Galtieri, M. Garcia-Sciveres, J. Lys, W. M. Yao Study Of Soft Gluon Radiation In W+Jets Events, CDF/PHYS/TOP/CDFR/3253. We thank the L. Galtieri for making this available to us.

[22] See for the file locations:

`http://www-cdf.fnal.gov/internal/physics/top/w_mc_samples.txt`

[23] S. Kuhlmann, *Timing Information For Central Photons and the $ee\gamma\gamma\not{E}_t$ Event*, CDF note 4256, July 1997

[24] H. J. Frisch, *A Filter for 'One-legged' Cosmic Ray Muons in Run IB Data*, CDF note 4830.

[25] See Figure 4.4, page 69, of D. Toback, Ph.D. thesis, University of Chicago, 1997.

[26] J. Berryhill, R. Culbertson, C. Grosso-Pilcher, P.J. Wilson, H.J. Frisch, *Photon Selection for Exotic Analyses* CDF/ANAL/EXOTIC/CDFR/4580, May, 1998

[27] A. Scott, J. Hauser, D. Saltzberg, P. Murat, *An Effective Cosmic Ray Filter for Run 1 Dimuon Analyses*; CDF/ANAL/ELECTROWEAK/CDFR/4755 This sample is a loose cosmic sample; the muon selection cuts are much weaker than those of the final filter. Only the cuts in Table 2 of A. Scott, Y. Bonushkin, J. Hauser, D. Saltzberg, *Low Mass Drell-Yan Cross Sections from Run IB Data* CDF/ANAL/ELECTROWEAK/CDFR/4539 were applied. In particular, cuts on invariant mass ($11 < M < 600$), isolation (track and cal summed in quadrature < 2 GeV), Z vertex (< 60 cm), trigger path, and the requirement that the tracks be oppositely charged have not been applied. We apply the cuts described in CDF4380 to clean up the sample. We thank Andrew Scott for providing this really nice loose sample.

[28] The $Z^0 \to \mu^+\mu^-$ and $W^\pm \to \mu^\pm\nu$ samples are described in $http://hep.uchicago.edu/cdf/ntuple\_datasets.html$.

[29] D. Smith and H. B. Jensen, *Pion Punchthrough Probability in the Central Calorimeter*, CDF/ANAL/MUON/CDFR/707. August 1988. This is a careful job that compares test-beam data on a wedge with predictions from measured pion and kaon cross-sections.

[30] B. Denby and M. Contreras, *A New Look at Punchthrough at CDF*, CDF/MEMO/MUON/CDFR/1324, Nov. 1990. This uses the dependence of the number of absorption lengths as a function of rapidity to estimate punchthrough.

[31] B. T. Huffman, J. Suzuki, P. Singh, S. Kim, E. Engels Jr., and P. Shepard *The Discovery of the B_c Meson* CDF/ANAL/BOTTOM/CDFR/3991, Oct, 1997. The code used is an updated version of Dave Smith's CMWINT program, CMWINT.CDF.

[32] Tsuyoshi Nakaya, private communication. This uses identified pions from D^* decay to calibrate the punchthrough rate.

[33] These events are stored in PAD format in the files UCCDFL$DKA500:[DATA.CDF.ANA.JWB]JGHIBIT_JGHIBi.PAD, where i runs from 1 to 9, and JGHIBIT_WGHIBi.PAD, where i runs from 1 to 3.

[34] J. Berryhill, Ph.D thesis, Univ. of Chicago, in preparation.

[35] J.W. Cronin et al., *Production of Hadrons at Large Transverse Momentum at 200, 300 and 400 GeV*, Phys. Rev. **D11**, 3105 (1975); *Production of Kaons, Protons and Antiprotons with Large Transverse Momentum in p-p and p-d Collisions at 200, 300, and 400 GeV*, Phys. Rev. Lett. **38**, 115 (1977); *Strange Sea and alpha(s) measurements from neutrino n deep inelastic scattering at CCFR NUTEV*. By CCFR NuTeV Collaboration (Jaehoon Yu for the collaboration). FERMILAB-CONF-98-198-E, Mar 1998. 6pp. Talk given at 33rd Rencontres de Moriond: QCD and High Energy Hadronic Interactions, Les Arcs, France, 21-28 Mar 1998. e-Print Archive: hep-ex9806030

[36] While it's unlikely that all tracks are kaons, both Jon Rosner and Hitoshi Murayama have suggested that there could be anomalous production of kaons, either from charm or through processes such as the 'Compton' diagram $g + s \rightarrow \gamma s$.

[37] Selections used for inclusive high-Pt muon dataset are described at http://hep.uchicago.edu/cdf/inclusives.html. Note that the CMP is nowhere required in the trigger or other selection criteria.

[38] Rowan Hamilton, *Measurement of Photon-Charm Production in $\bar{p}p$ Collisions at $\sqrt{s} = 1.8$ TeV*, CDF/PHY/CDFR/4752; ibid. Ph.D.Thesis. (Harvard U.). UMI-97-10424-mc (microfiche), 1996;

[39] Koichi Kurino, Steve Kuhlmann, *A Measurement of The Photon + Muon Cross Section For RunIB.* CDF/ANAL/JET/CDFR/4822

[40] A. Scott, *Measurement of the W Boson Mass with the Collider Detector at Fermilab*, Ph.D thesis, Harvard U., Nov. 1988. We thank Mark Lancaster for this reference and help.

[41] See http://hep.uchicago.edu/cdf/zeeflt.html.

[42] CDF-2699, Sample selection for Run IB Top Search